Eloise Cu-Au-Ag deposit

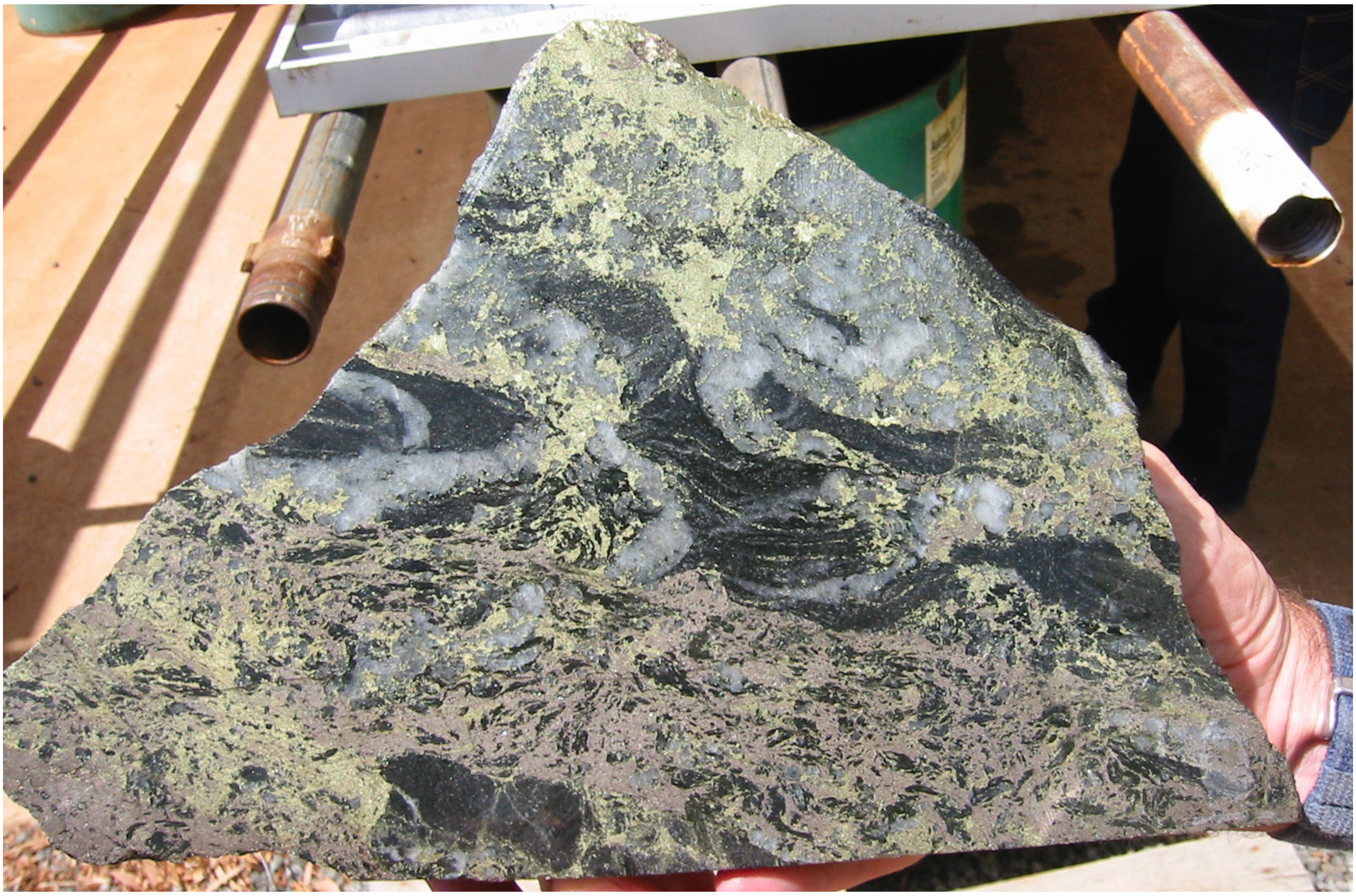

LOCATION

Geological Domain

Eastern Fold Belt/Soldiers Cap Domain (Maranon Supergroup; Beardsmore et al., 1988; Figs. 7.1 and 7.2)

Co-ordinates

Latitude: 20° 49' 58" S
Longitude: 140°50 55" E

MGA Zone 54: 497,700 E; 7,681,821 N

NATURE OF MINE

Mined Commodities

Cu, Au, Ag

Mining Method

Underground long hole stoping at 25 m mine level spacing (until 2008) and longitudinal sub-level caving (2011 to present)

Depth of Mining

>1,000 m

PRODUCTION AND DIMENSIONS

Mineralised bodies

The Eloise deposit has a strike length of over 1,000 m and is mineralised to a depth of over 2,000 m (Fig. 7.7). Mineralisation occurs broadly in western and eastern lenses, separated by approximately 150 m of amphibolite (Fig. 7.6 and Fig. 7.7; Baker, 1996; Hodkinson et al. 2003). A series of post-mineralisation faults have dislocated the mineralisation into disparate, steeply dipping/plunging lodes and lenses which extend to depths >1,000 m (Figs. 7.8 and 7.9).

Dimensions

The Elrose Lode and Levuka Lode described by Baker (1996, 1998) and referred to as the A and B Lodes respectively, by Hodkinson et al (2003; Tables 1 and 2; Figs. 7.6 to 7.8) are the main mineralised lodes of the original Eloise discovery. The Elrose and Levuka Lodes are subparallel and range from 180 to 240 m in strike length and 6 to 25 m in width with a vertical extent ranging between 700 and more than 1,000 m (Hodkinson et al., 2003). The southern extension of the Levuka Lode constitutes the Eloise Deeps where mineralisation extends to more than 1,000 m below surface (Warren et al. 2016).

Eloise Northwest, Eloise West (62 Lode) and the 40 Lode, located in the Western Arenite (Figs. 7.6 to 7.9), form part of a weakly mineralised structural corridor over 800 m in length and 200 m wide which contains localised domains of economic grade mineralisation (Hodkinson et al. 2003). The Western Arenite is separated from the Elrose and Levuka Lodes by an amphibolite body approximately 150 m wide (Fig. 7.7). The Middlewest and Lower Midwest ore bodies are also located within the Western Arenite (Figs. 7.8 and 7.9; Tables 7.1 and 7.2).

Orientation of Mineralised bodies

The Elrose and Levuka Lodes are sub-parallel forming vertical/sub-vertical (east dipping), steeply plunging (60-75°) ore domains with a N to NNE trend (Baker, 1996). Eloise West and Eloise Northwest Lodes are also N-trending and steeply east dipping but with no apparent plunge to the ore lodes (Hodkinson et al. 2003). Eloise Deeps is a sub-vertical, N-trending down plunge extension of the Elrose-Levuka Lodes below the Ramsey Fault (Warren et al., 2016). Chloe is a sub-parallel low grade lens, separated by a fault, structurally located below the Elrose-Levuka Lodes (Fig. 7.8; Warren et al. 2016). The orientation of these lenses are not documented, but sections from 3D wireframes in Warren et al. (2016) suggest they are sub-parallel to the N-NNE trending Elrose-Levuka Lodes and plunge steeply (60-75°) towards the south. A summary of known lenses are tabulated in Tables 7.1 and 7.2.

Historic Production

Amalg Resources NL (1995-1996) 1,220 tonnes Cu, 0.4 tonnes Ag and 16 kg Au (Wallis et al., 1998).

Breakaway Resources Ltd (2002-2003) 551,590 dry tonnes at 3.85 % Cu and 0.97 g/t Au for 20,265 tonnes Cu; 9,404 ounces Au and 207,797 ounces Ag (Breakaway Resourc-

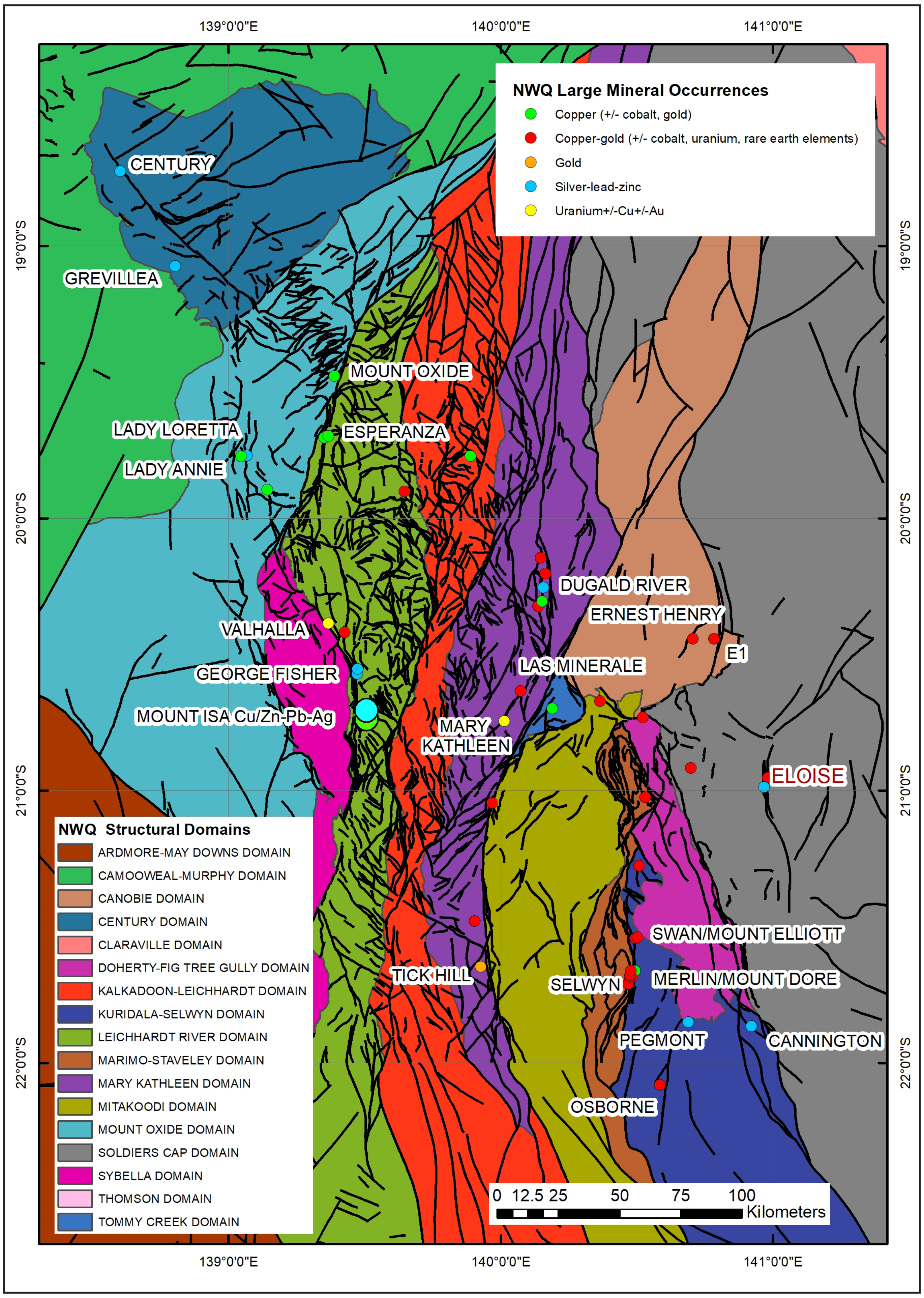

Figure 7.1. Regional location of Eloise shown with respect to the Soldiers Cap Structural Domain Map from the 2010 NWQMEP GIS

The most current resource estimate for Eloise released by FMR Investments is 2.3 million tonnes at 2.1 % Cu (Warren et al. 2016).

RESERVES

Breakaway Resources Ltd released a proved and probable reserve estimate of 0.93 Mt at 3.97 % Cu in 2003 (Breakaway Resources Ltd, 2003; Hodkinson et al. 2003). No updated reserve estimates have been released.

TOTAL IN SITU METAL

Based on the most recent resource estimate (Warren et al. 2016), Eloise contains approximately 46,800 tonnes of copper metal.

HOST ROCKS

Mine Stratigraphy

The Eloise deposit is hosted by the Mount Norna Quartzite which forms part of the Soldiers Cap Group within the Proterozoic Eastern Fold Belt of the Mount Isa Inlier (Fig. 7.1). The Mount Norna Quartzite at Eloise comprises a sequence of arenitic metasediments, amphibolites and quartz biotite schists (Beardsmore et al. 1988; Baker, 1996; Baker and Laing, 1998). The mine sequence comprises near vertical units interpreted to represent the eastern limb of the Middle Creek Antiform (Hodkinson et al. 2003).

An unmineralized, locally gneissic garnetiferous psammite occurs in the far east of the deposit (Fig. 7.4; Baker, 1998) forming a north striking unit which is regionally correlated with the Fullarton River Group (Beards-

es Ltd, 2003).

FMR Investments production at Eloise for 2007-2008 was 391,787 dry tonnes for 9,673 tonnes Cu (Breakaway Resources, 2008).

Recent Production

Current production and milling averages 60,000 tonnes per month to produce 4,300 tonnes of concentrate at an average grade of 27 % Cu (equivalent to 1,160 tonnes Cu; fmrinvestments.com.au). No data is currently available for recent Au and Ag production.

RESOURCE

The original pre-mining resource was 3.1 Mt @ 5.5 % Cu, 1.4 g/t Au and 16 g/t Ag (Baker, 1998).

Estimates by Minotaur Exploration Ltd indicate that the Eloise system contained a pre-mining original resource of 10 Mt at 3.2 % Cu and 0.7 g/t Au (DNRME, 2017).

Table 7.1. Ore bodies/lodes of the Eastern part of the Eloise Mine sequence (Refer Fig. 7.8)

	Lode/Orebody	Strike Length (m)	Width (m)	Vertical Extent (m)	Trend/plunge
Eastern Lodes	Elrose (A Lode)	180	6 to 20	120	NNE-strike; vertical to SE dip 65-75° plunge SW
	Levuka (B Lode)	200 - 240	18 - 25	160	NNE-strike; vertical to SE dip 65-75° plunge SW
	Levuka South	200	25	>300	NE-strike; Vertical to SE dip
	Eloise Deeps	>700	50	>1,000	NE-strike; Vertical to SE-dip; >80° plunge SW
	Chloe	250	<5	250	NE-Strike; Vertical
	42 Lodes	170	<10	150	NNE to NE; Vertical dip; >80° plunge SW

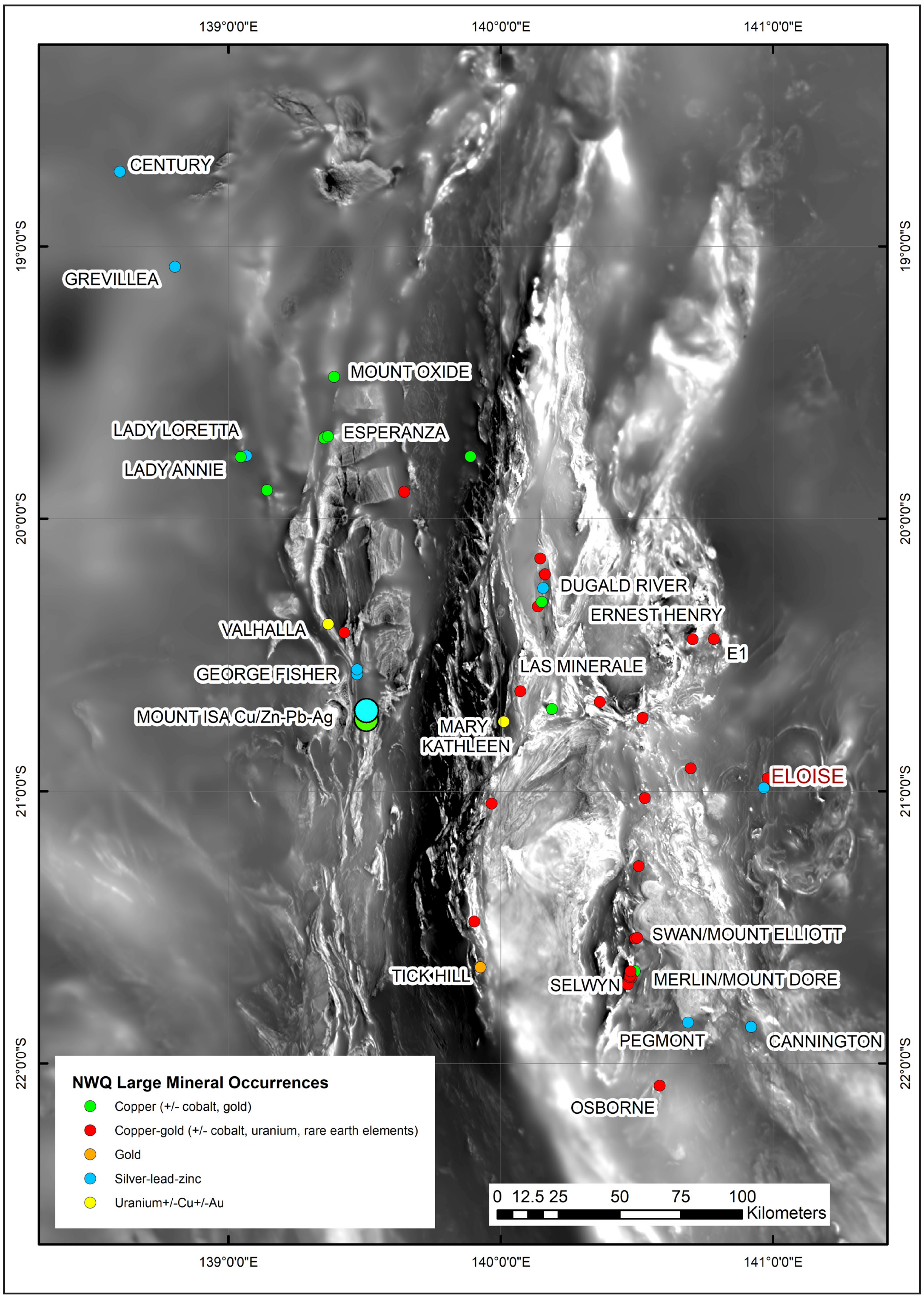

Figure 7.2. Regional location of Eloise overlain on an image of total magnetic intensity from the GADDS data for the region

more et al. 1988). A domain of quartz-biotite and quartz-muscovite schists, termed the Eastern Sequence by Hodkinson et al. (2003), occurs to the west of the garnetiferous psammite. This barren unit grades into the host arenite sequence to the west. West of the host arenite is a texturally homogenous, medium- to coarse-grained amphibolite unit with inferred chilled margins potentially indicating an intrusive origin (Hodkinson et al. 2003; Fig. 7.3). The amphibolite is approximately 150 m and separates the highly mineralised host arenite in the east from the more weakly mineralized lodes hosted by the western arenite (Hodkinson et al. 2003; Fig. 7.3).

The Proterozoic basement hosting the Eloise deposit is unconformably overlain by a 50 to 70 m thick sequence of Cretaceous mudstone, siltstone and sandstone of the Willumbilla Formation, and Tertiary fluvial sediments (Robertson and Shu, 2003).

Major Host Rock

The major host rock sequence at Eloise is termed the host arenite (Fig. x.2) which contains the Elrose-Levuka, Chloe (and The Dead Horse) and the Eloise Deeps lodes (Hodkinson et al. 2003. Hodkinson et al. (2003) describe the host arenite as comprising fine to medium grained biotite-rich, massive to locally schistose micaceous meta-arenites. Baker and Laing (1998) document the Elrose Lode as being hosted by meta-arkose units whereas the Levuka Lode is hosted by quartz-biotite schists (Fig. 7.3). A distinctive banded magnetite-carbonate unit occurs along the western margin of the Levuka Lode is documented by Hodkinson et al. (2003) which may be up to several metres in width.

Minor Host Rock

The Eloise Northwest, Eloise West (62 Lode), 40 Lode, Middle West and Lower Middle West lodes are hosted by a meta-arkose unit (Baker, 1998) termed the western arenite by Hodkinson et al. (2003). This occurs to the west of the amphibolite unit, which separates the eastern lodes from the lower grade western lodes (Fig. 7.3). The western arenite comprises weakly foliated to massive fine- to medium-grained siliceous meta-arenites (Hodkinson et al. 2003) or meta-arkose (Baker, 1998). Where present, the foliation in the western arenite is defined by mafic alteration patches which locally intensify to form horizons of economic magnetite-carbonate-chalcopyrite-pyrrhotite (Hodkinson et al. 2003).

Table 7.2. Ore bodies/lodes of the Western part of the Eloise Mine sequence (Refer Fig. 7.8)

	Lode/Orebody	Strike Length (m)	Width (m)	Vertical Extent (m)	Trend/plunge
Western Lodes	40 Lode	120	<10	70	N-strike; Vertical dip; 30° plunge S
	Eloise West (62 Lode/Middle West)	150	8.5	100	N-strike
	Macy	300	10	250	NNE-strike; Steep dip W
	Emerson/Sheila	500	20	300	NE-strike; Vertical to >75° Plunge
	Eloise North West	90	5	100	N-strike

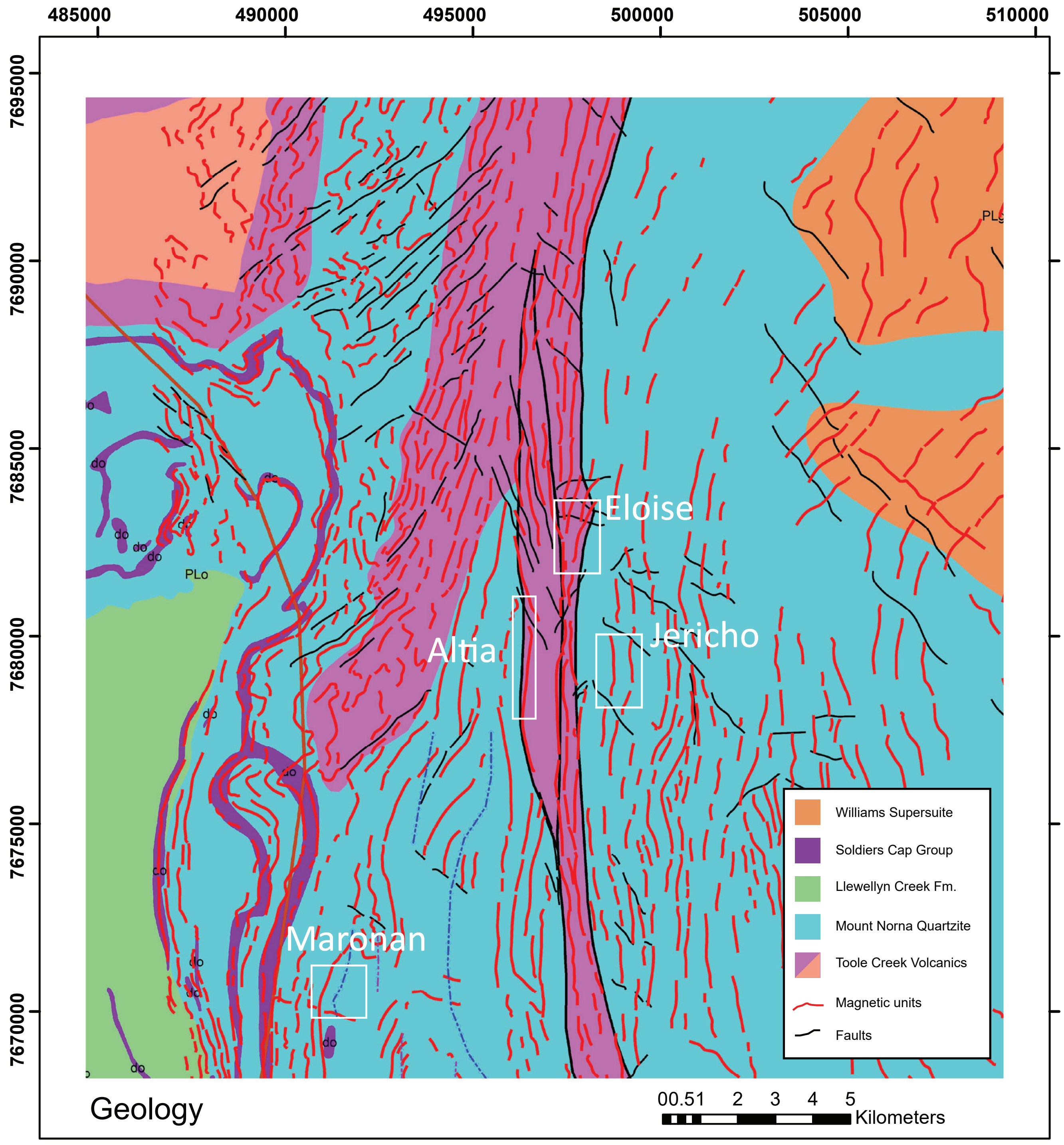

Figure 7.3. Regional geological map of bedrock solid geology from NWQMEP compilation (2010).

Magnetic susceptibility and Inductive EM conductivity

Brescianini et al (1992) reported high Magnetic Susceptibility in magnetite-rich altered rock units (1.3 SI), decreasing to 0.5 and 0.25 SI in mafic schists and massive sulfides respectively (Table 7.3). Stockwork veined mafic units have higher magnetic susceptibilites (0.04 SI) than both the micaceous meta-arenite and siliceous meta-arenite (0.001 and 0.0006 respectibly). The regionally extensive amphibolite unit has a Magnetic Susceptibility of 0.0004 SI, slightly higher than surrounding micaceous quartz schists (0.0001 SI; Brescianini et al (1992).

Mineralised units have high inductive conductivities between 2,000 and 3,000 S/m in the stockwork ore and massive sulphides respectively (Brescianini et al.1992). Magnetite -rich carbonate altered units have Inductive EM Conductivity of 25 S/m in contrast to all other host units which have negligible conductivities (Table 7.3).

INTRUSIVE ROCKS IN REGION

Granitoids

No granitic intrusive rocks have been encountered in the drilling at Eloise. Regional gravity data from Morse et al. (1992) reveals a broad (15 km x 7 km) ellipsoid-shaped gravity low occurs to the northeast of Eloise. Baker (1998) suggests that this may be an intrusive pluton related to the 1520-1490 Ma Williams batholith (e.g., Wyborn, 1990).

Amphibolites

Amphibolite units occur in the Eloise mine sequence (see above) are interpreted to have a mafic intrusive origin (Baker, 1998; Hodkinson et al., 2003). These units are identified in regional magnetic data (Fig. 7.2) and in mine deposit studies (Fig. 7.3).

PETROPHYSICAL PROPERTIES

Density

Brescianini et al (1992) documented a range in densities for rock units in the deposit from 2.71 g/cm³ for schists and arenites, to 3.96 g/cm³ for massive sulphides and magnetite altered rocks (Table 7.3).

Table 7.3. Petrophysical determinations of major rock types at Eloise. Modified from Brescianini et al (1992).

Rock Type	Volume %	Magnetic Susceptibility (SI)	Density (g/cm³)	Inductive EM conductivity (S/m)
Magnetite-carbonate altered rock	2-5 % po 50-60 % mt	1.3	3.96	25
Amphibolite	<1% py + cpy	0.0004	2.75	Slight
Micaceous quartz-schist	-	0.0001	2.71	0
Micaceous meta-arenite	<1% py + cpy	0.001	2.73	Slight
Siliceous meta-arenite	1-2% cpy	0.0006	2.56	0
Mafic schist	2-5% po + cpy	0.5	3.18	1
Stockwork veined mafic	10-20% po 5-10% cpy	0.04	3.23	2,000
Massive sulfide	20-40% po 40-60% cpy	0.25	3.95	3,000

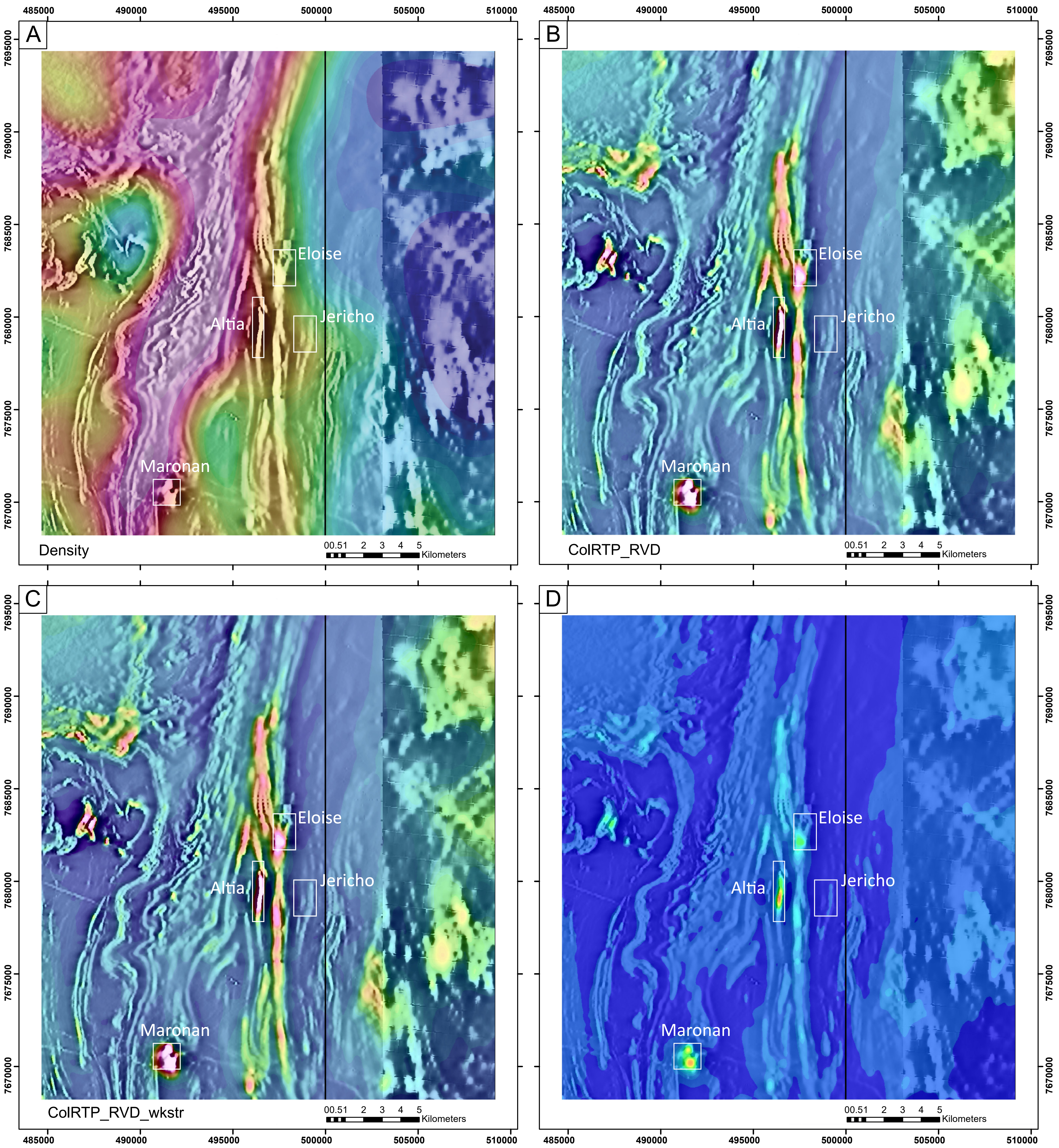

Figure 7.4. Regional geophysical expression of Eloise and surrounding deposits. A) Apparent density calculation from government gravity calculation. B) Airborne total magnetic intensity reduced to pole (RTP). C) Airborne magnetic intesity (RTP, vertical derivitive). D) Airborne magnetic intensity (RTP, linear stretch maintaining original pixel values).

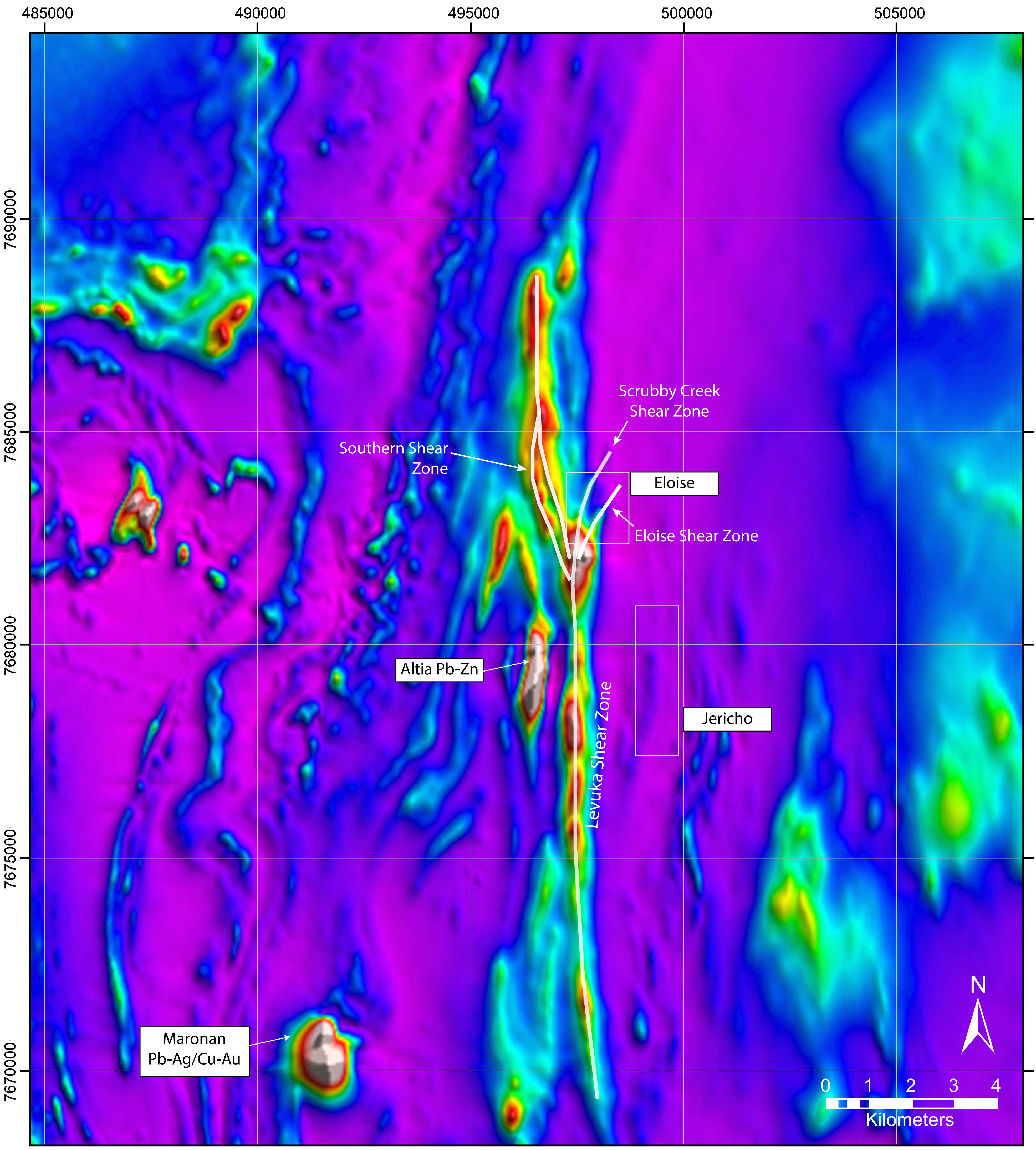

Figure 7.5. Total magnetic intensity reduced to pole (RTP) map and structural interpretation from Baker (1996). Map projection MGDA94/MGA54

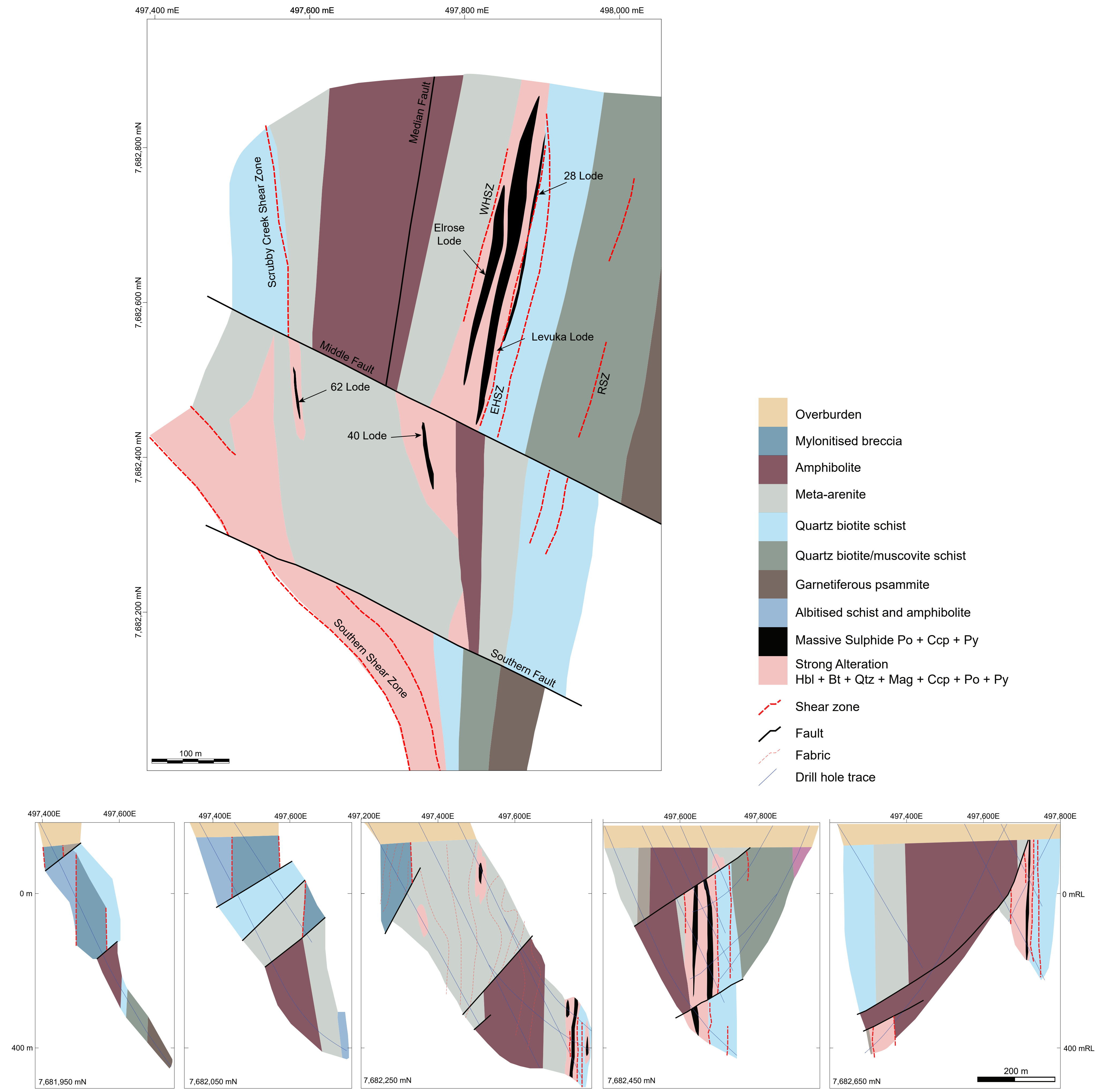

Figure 7.6. Geological plan map at -100 mRL and geological cross-sections redrawn from Baker (1996).

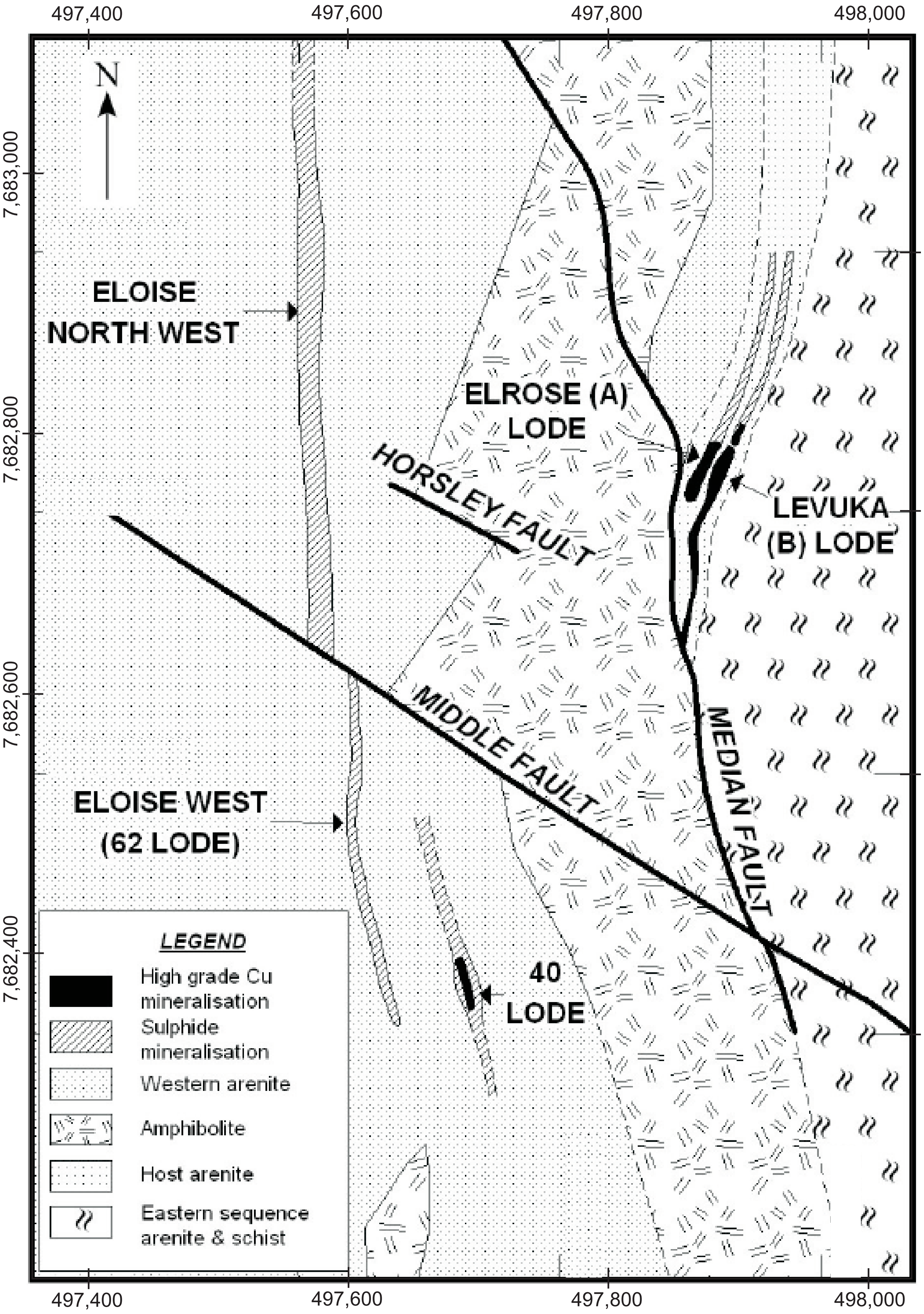

Figure 7.7. Solid geology plan map at -100 mRL modified from Hodkinson et al (2003).

METAMORPHISM

Metamorphic Grade

Baker and Laing (1998) indicate that host sequences were metamorphosed to an assemblage of hornblende + andesine + quartz in the amphibolite and quartz + biotite + staurolite + andalusite + garnet in the metasediments indicating prograde metamorphic conditions of 550-600 °C and pressures <350 MPa (Spear and Cheney, 1989; Bucher, 1994).

STRUCTURAL CHARACTERISTICS

Structural Setting

The Proterozoic host rocks to the Eloise deposit are concealed below the western margin of the Eromanga Basin. Consequently, the regional structural setting has largely been interpreted from ground and aeromagnetic surveys, drill core observations and deposit modelling (Brescianini et al., 1992; Baker and Laing, 1998; Hodkinson et al. 2003; Warren et al. 2016).

The regional structural history includes early extension (Holcolmbe et al. 1991) followed by main stage compressional events related to the Isan Orogeny (1,620-1,500 Ma). The main phases include D_1 north-south compression and associated thrusting and faulting (Baker and Laing, 1998). Major east-west compression during D_2 generated N-S trending upright folds followed by D_3, an E-W compressive event producing N-NE trending folds (Baker, 1998; Baker and Laing, 1998). Peak metamorphism occurred during D_2 (1,584 Ma; Page and Sun, 1996).

Eloise is located within a regionally-extensive, north-trending, sub-vertical shear zone termed the Levuka Shear Zone (Fig. 7.5; Newbery, 1990; Baker and Laing, 1998) which coincides with a major north-trending regional magnetic feature termed the Levuka trend (Skrzeczynski, 1993; Fig. 7.5). The Levuka Shear Zone is located on the eastern limb of the Gold Reef Dam Synform which is likely a D_2 structure based on the tightness of the fold and the north-south strike (Baker and Laing, 1998).

STRUCTURAL HISTORY

Major Structural Styles

The regional Levuka Shear Zone imposed a strong structural control on the location of the Eloise deposit which demonstrates a high degree of local complexity including a series of anastomising shears (Fig. 7.5; Baker and Laing, 1998). In the region of the Eloise deposit, the Levuka Shear Zone comprises a series of north-northwest and north-northeast striking shear zones with sub-vertical to vertical dips. These include the north-northwest trending Southern Shear Zone (SSZ), which diverges from the north-northeast trending Eloise Shear Zone (ESZ) and the north-northeast trending Scrubby Creek Shear Zone (SCSZ) (Figs. 7.5 and 7.6; Baker and Laing, 1998). In the region of Eloise, these splays form a lozenge shape which is coincident with the regional magnetic anomaly and interpreted to represent a dilational jog feature (Baker and Laing, 1998). North of Eloise, the shear zones reconverge to form the northern trend of the regional Levuka Shear Zone (Fig. 7.5).

Nature and Orientation of Controlling Structure

The Eloise deposit is bound to the east by the Eloise Shear Zone and the south/southwest by the Southern Shear Zone and the Scrubby Creek Shear Zone to the northwest (Fig. 7.5; Baker, 1996). In the region of the Eloise deposit, the Eloise Shear Zone comprises the Western Host Shear Zone (WHSZ), the Eastern Host Shear Zone (EHSZ) and the Retrograde Shear Zone (RSZ; Fig. 7.6; Baker and Laing, 1998). Baker (1998) and Baker and Laing (1998) indicated that the Southern Shear Zone contains minor sub-economic mineralisation associated with planar veins containing pyrite and chalcopyrite. Similarly, the Scrubby Creek Shear Zone contains sub-economic pyrrhotite-rich mineralisation along its margin (Baker and Laing, 1998).

The Elrose (A Lode) and Levuka (B Lode) Lodes are located within the Eloise Shear Zone. The Elrose Lode is bounded on its western margin by the Western Host Shear Zone (WHSZ) which comprises strained albite-hornblende alteration with stock work veins and massive sulphide lenses (Baker, 1996). The Eastern Host Shear Zone (EHSZ) bounds the eastern margin of the Levuka Lode and represents a high strain zone up to 50 m thick (Baker and Laing, 1998). The EHSZ comprises foliation parallel boudinaged quartz veins

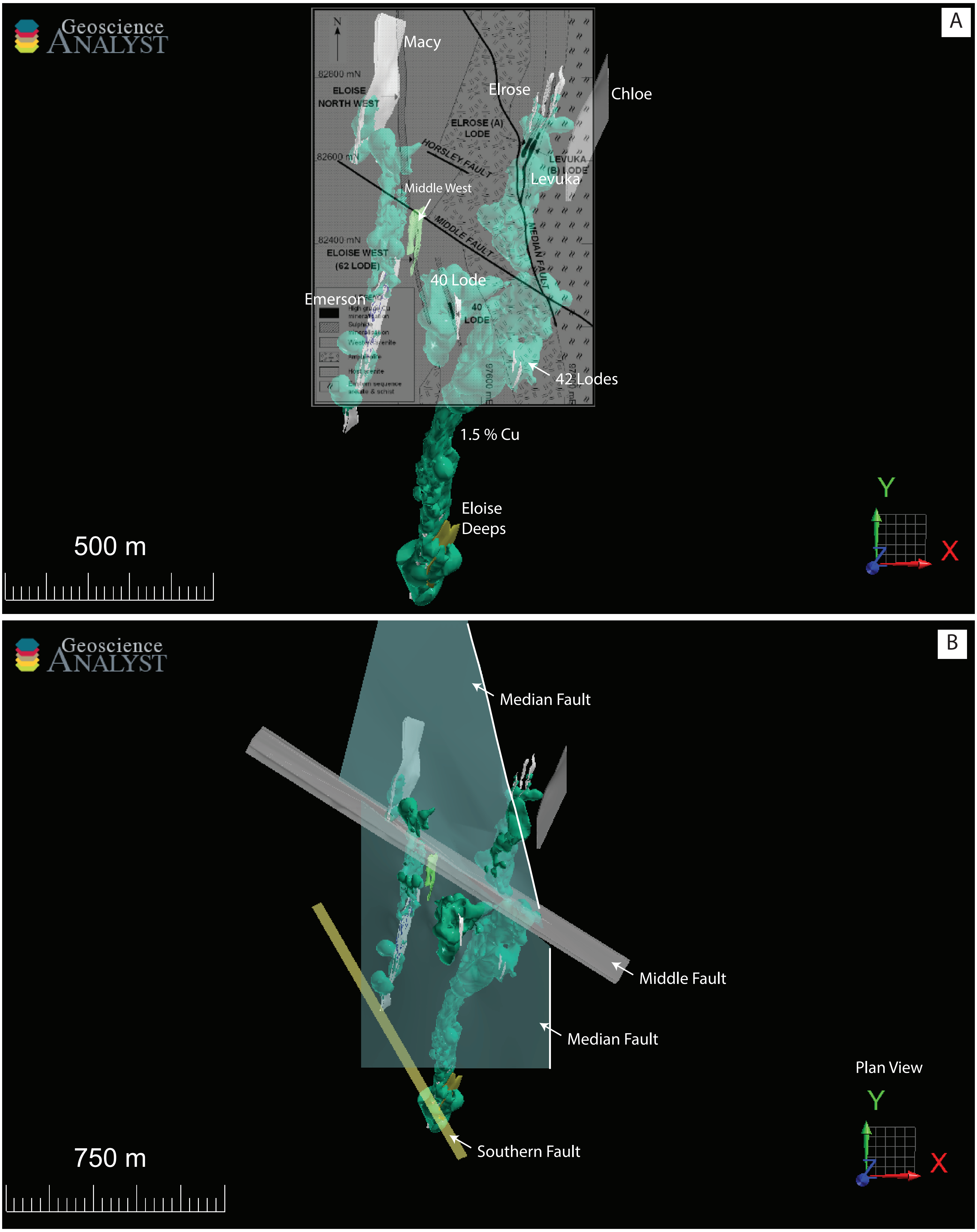

Figure 7.8. Eloise ore lenses and 1.5 % Cu interpolent grade shell (from Leapfrog model) shown in A. Major structures are shown in B. Ore shell and fault wireframes provided by FMR Investments.

Figure 7.9. Oblique view of Eloise ore lenses and 1.5 % Cu interpolent grade shell (from Leapfrog model) shown in A with plan geology map of Hodkinson et al. 2003. Major structures are shown in B. Ore shell and fault wireframes provided by FMR Investments.

hosted by quartz-biotite schist and massive sulphide lenses. The relative timing of mineralisation is interpreted by Baker and Laing (1998) to be synchronous with the transformation from ductile to brittle deformation (D_2 to D_3) during the waning stages of the Isan Orogeny (1,540-1,500 Ma).

Post Mineralisation Structure

Brittle D_3 deformation caused structural offset of the lower part of the Levuka Lode at a level around -350 mRL by the Median Fault to offset the Levuka Lode and Eloise Deeps (Fig. 7.8 and 7.9; Baker and Laing, 1998). The Median Fault trends north with a moderate to steep westerly dip with a separation of up to 100 m in cross section. At the margins of the fault zone, calcite-chlorite veins occur in the host rock

The upper parts of the Elrose and Levuka Lodes are offset by the Middle Fault (Fig. 7.8 and 7.9), a west-northwest trending, steeply dipping structure which displays 50-100 m of sinistral horizontal movement and 20 – 100 m of vertical displacement (Baker and Laing, 1998). The Middle Fault has offset the Eloise Shear Zone, the Median Fault, the amphibolite unit and magnetic contours (Fig. 7.9; Baker and Laing, 1998).

Both the Middle and Median Faults comprise brecciated and silicified host rock clasts with a chlorite, calcite, pyrite and chalcopyrite matrix (Baker, 1996).

A number of additional faults have been identified and modelled by FRM Investments. These include the Lunney Fault (Fig. 7.9) a NW striking, SW dipping structure located below the Elrose and Levuka lenses and above the Chloe lense. The Ramsey Fault trends N-S and dips moderately to the west (Fig. 7.9) intersecting the upper part of the Eloise Deeps lense and off setting the western lenses including Emerson (Fig. 7.9B). Numerous other structures are included in the Geoscience Analyst compilation.

WALLROCK ALTERATION

General Characteristics

Regional albitisation is a characteristic feature of shear zones within the Mount Isa Inlier representing post-peak metamorphism but typically pre-dating mineralisation. Pervasive albitisation occurs at Eloise (e.g., Stage I albitisation; Baker, 1996; Fig. 7.10) replacing peak metamorphic assemblages. Rocks adjacent to the Southern Shear Zone and the amphibolite west of the main lodes have been variably albitised, including the Elrose Lode. However, the Levuka Lode and quartz-biotite schist to the east are not albitised. Baker (1998) describes a zone of strong Fe-Mg-K-Ca metasomatism (Stage II) comprising hornblende, biotite, quartz, magnetite and minor sulphides (pyrrhotite, chalcopyrite and pyrite) which overprinted early albitisation and formed veins and selvages.

Stage III alteration accompanied main-stage Cu-Au mineralisation (Fig. 7.10) and preferentially overprinted Stage II alteration assemblages through replacement of hornblende by calcite, chlorite, quartz, actinolite and sulphides including chalcopyrite, pyrrhotite and pyrite (Baker, 1996). Stage IV alteration and mineralisation is constrained to thin (0.5 to 5 cm) veins formed during the waning stages of mineralisation and are concentrated around shear zones and lodes (see below).

Inner (ore) zone

Alteration associated with the ore zones shows complex overprinting mineral associations. Early Stage I albitisation associated with shear zones is largely pervasively replaced by Stage II hornblende-biotite veins and replacements (Baker, 1998; Fig. 7.11A). Alteration intensity increases in the vicinity of the Elrose and Levuka ore lodes (Eloise Shear Zone) and the Southern Shear Zone (Fig. 7.11) where vein abundance and alteration affects more than 70% of the rock mass (Baker, 1998). Main stage mineralisation (Stage III) includes chalcopyrite-pyrrhotite-calcite-chlorite-quartz-magnetite veins (Fig. 7.10B) and semi-massive sulphide replacements/breccia infill of earlier alteration assemblages (Fig. 7.10C). The ore related alteration zone extends <50 m from the major mineralised lodes. The inner ore zone around Elrose, Levuka and 28 Lode north of the Middle Fault are characterised by chalcopyrite and pyrrhotite dominant mineralisation (Baker, 1998). Magnetite and pyrite abundance increase south of the Middle Fault, into an area with a relatively broad alteration footprint (300-400 m) and hosting only minor ore grade intercepts including the 40 Lode and the 62 Lode (Baker, 1998).

Outer zone

The alteration intensity diminishes with distance from the main lodes and major shear zones and Stage I albitisation is rarely observed in the wall rocks distal to these features (Hodkinson et al., 2003). Stage IV brittle veins occur throughout the deposit but are abundant adjacent to the lode zones forming an outer zone to the mineralisation. Baker (1998) recognised four vein sets including i) chlorite-K-Keldspar-calcite-muscovite-chalcopyrite-hematite; ii) K-Feldspar-tourmaline-cal-

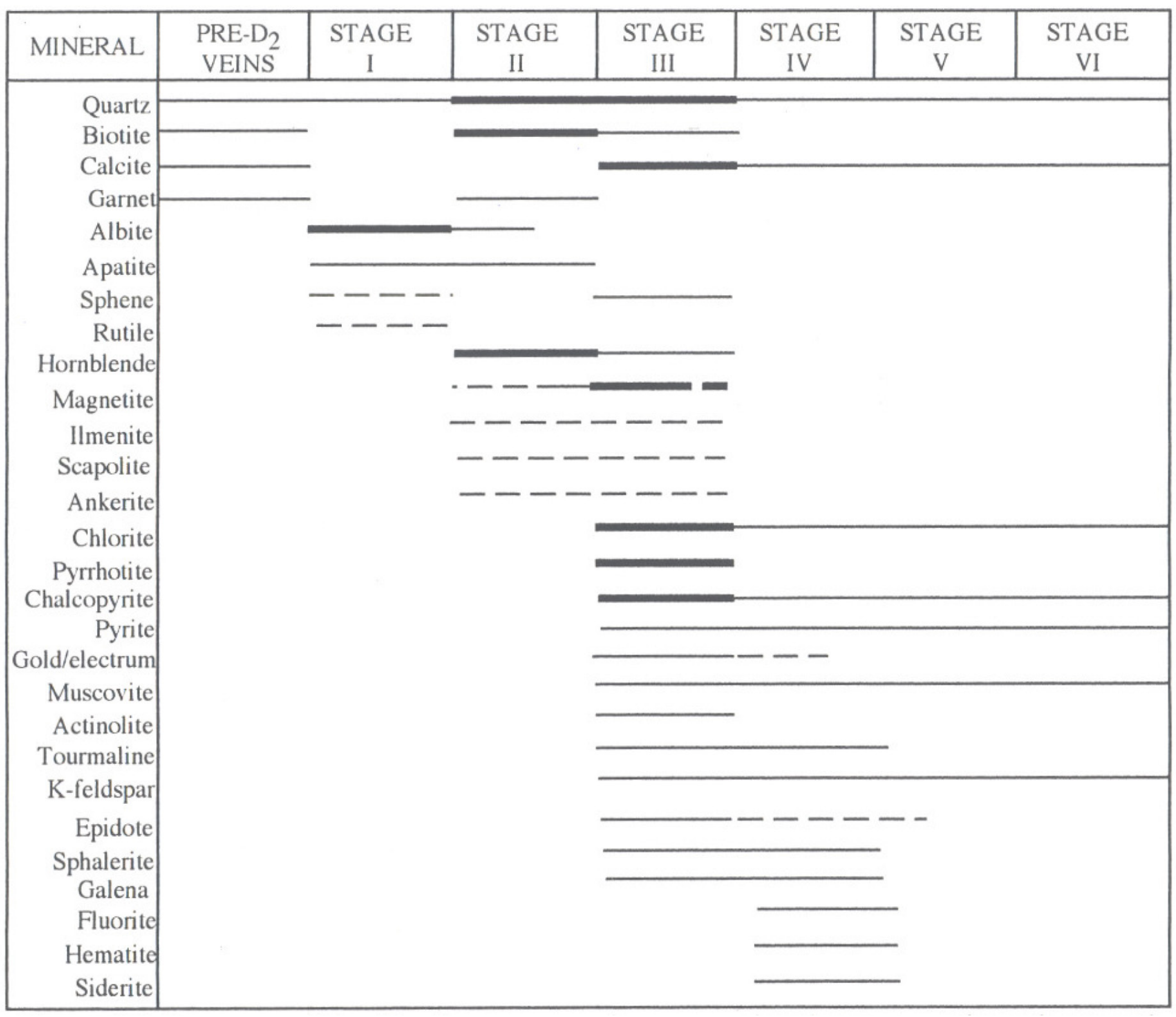

Figure 7.10. Summary of Eloise alteration paragenesis from Baker (1996). Thick black bars are major phases, thin black bars are minor phases. Dashed lines represent uncertain paragenetic timing including veins of stage IV.

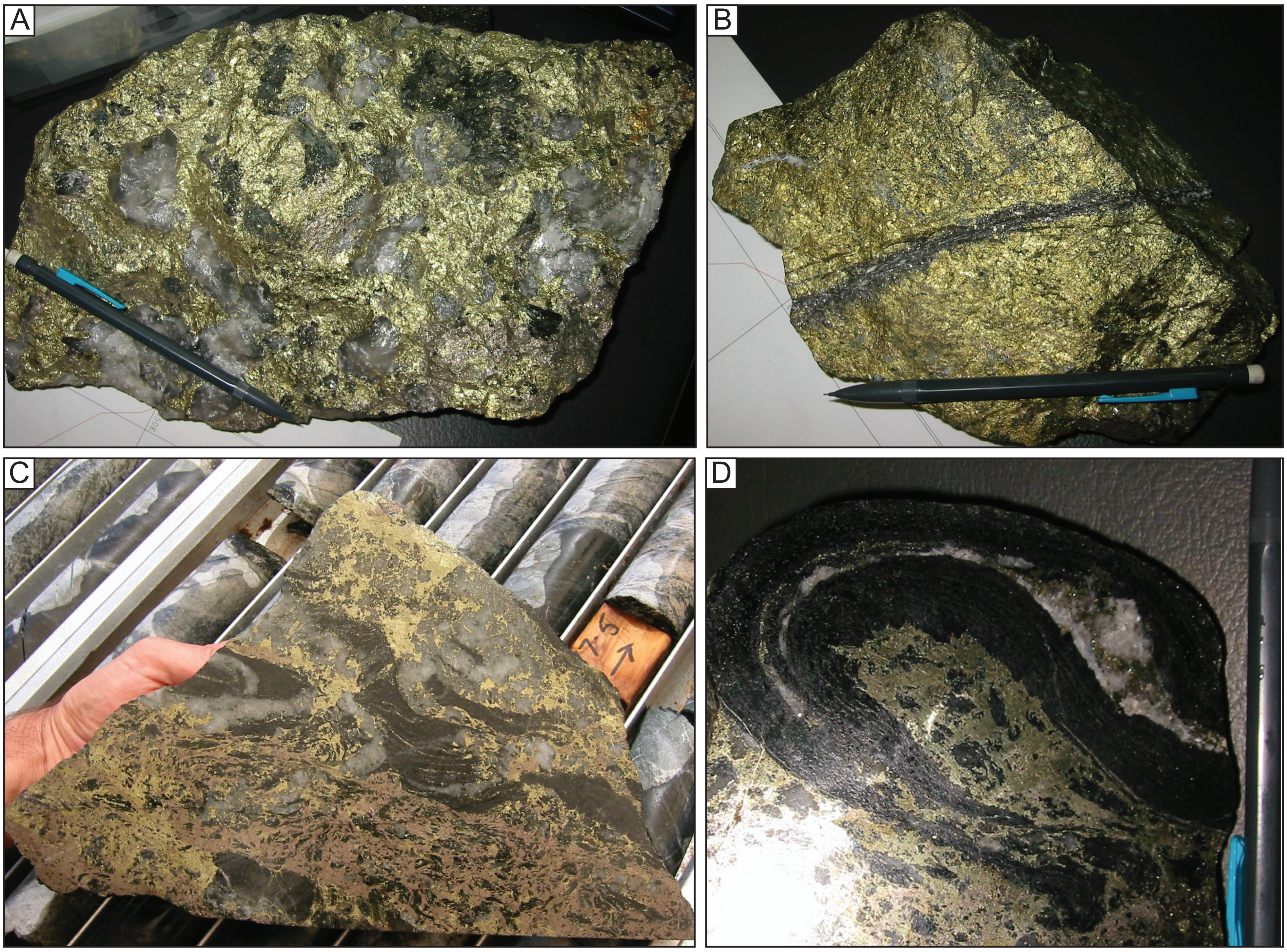

Figure 7.11 Hand specimens from Levuka and Elrose. A. Chalcopyrite-pyrrhotite infill texture associated with brecciation of earlier quartz veins and selective replacement of mafic-silicate alteration. B. Massive chalcopyrite-pyrrhotite ore with brecciated quartz veins cross-cut by magnetite-biotite veins. C. Mafic-silicate alteration of meta-psammite host rock with ductily deformed quartz veins and pyrrhotite-chalcopyrite selective pervasive alteration of earlier mafic-silicate assemblages. D. Highly ductily deformed quartz-sulfide vein with mafic-silicate alteration and selective pervasive replacement of the metapsammite host rock by pyrrhotite-chalcopyrite. Modified from Gow and Little, 2003.

cite-quartz; iii) siderite-hematite-pyrite; and iv) calcite-fluorite-K-Feldspar-muscovite-chlorite-sphalerite-galena-arsenopyrite-pyrite which only occur on the eastern margin of Levuka Lode. Stage IV veining and alteration is associated with replacement of albite by K-feldspar and hornblende/biotite by K-Feldspar causing a bleached colouration in amphibolite units (Fig. 7.10; Baker, 1996). The outer alteration zone (or moderate alteration, 30-70%; Baker, 1998) extends up to 100 m outboard of the inner (strong alteration zone; >70 %) and adjacent to the lower grade Eloise Northwest ore lenses (Baker, 1998; Hodkinson et al., 2003). This Northwest outer zone is dominated by pyrrhotite and restricted alteration halo of <20 m broadly confined to the eastern margin of the Scrubby Creek Shear Zone (Baker, 1998).

EXPLORATION GEOCHEMISTRY

The Eloise deposit is blind to the surface and has only a limited footprint in the cover sedimentary sequences directly overlying the deposit. Sampling and analysis of the Cretaceous sedimentary units above the unconformity directly overlying the Eloise deposit indicate anomalous Cu (75 ppm), Au (90 ppb) and As (125 ppm) within several metres of the unconformity (Robertson and Lui, 2003). In a more distal drill hole, 3 km from the Eloise deposit, the Cu (75 ppm), Au (26 to 56 ppb) and As (102 ppm) are similarly anomalous 1 m above the unconformity surface (Robertson and Lui, 2003). No pre-mining base line soil geochemistry sampling data is available for the Eloise deposit however, Hannen et al. (2018) report the results of a 2009 surface soil sampling campaign by X-Strata at the Eloise mine site which in part reflect contamination from airborne dust and mining operations (Hannan et al. 2018).

LITHOGEOCHEMISTRY

The Eloise drill hole data base does not include a comprehensive suite of elements making it largely unsuitable for comprehensive lithogeochemical analysis. Baker (1998) analysed a suit of samples using XRF and Neutron Activation Analysis (NAA). An example downhole plot from END019 is shown in Figure 7.14 with corresponding geochemical data from Baker (1998).

Four drill holes were analysed by the DNRME in 2019 using a TruScan^{TM} automated X-Ray Fluorescence core analyser. These drill holes (EAM127, EAM 128, EAM 130 and EAM 194) are located between major miner lodes (Fig. 7.15) but locally intercept highly mineralised zones. Down hole plots of three of these holes are shown in Fig. 7.16.

Figure 7.12 (Opposite page) Drill core photos from Levuka (B Lode). A. Strong biotite-hornblende alteration of metapsammite host rocks with fracture infill chalcopyrite mineralisation and ductily deformed calcite veins. B. Biotite-hornblende altered metapsammite cross cut by a fractured quartz vein with chalcopyrite-pyrrhotite-chlorite fracture infill. C. Chalcopyrite mineralisation likely formed as selective replacement of earlier hornblende-rich mafic-silicate alteration. White carbonate also occurs adjacent to the mineralisation. D. High-grade chalcopyrite mineralisation intergrown with pyrrhotite formed by replacement of earlier mafic-silicate alteration. Note fragmented quartz veins. This texture has been described as a 'durchbewegung' ore. E. Pyrrhotite - chalcopyrite dominated assemblage with abundant relict fragments of brecciated quartz veins. Modified from Gow and Little, 2003.

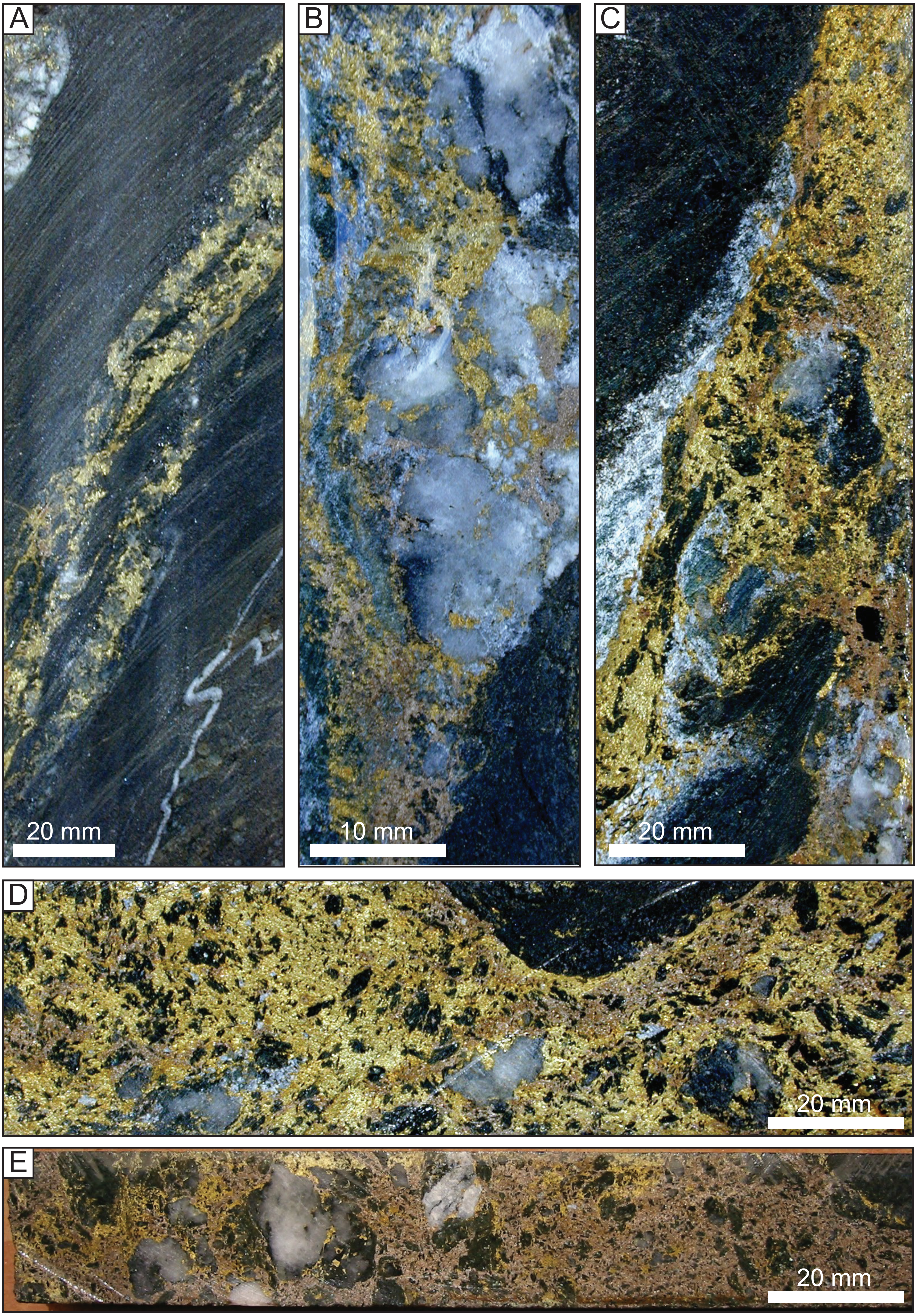
A
20 mm
B
10 mm
C
20 mm
D
20 mm
E
20 mm

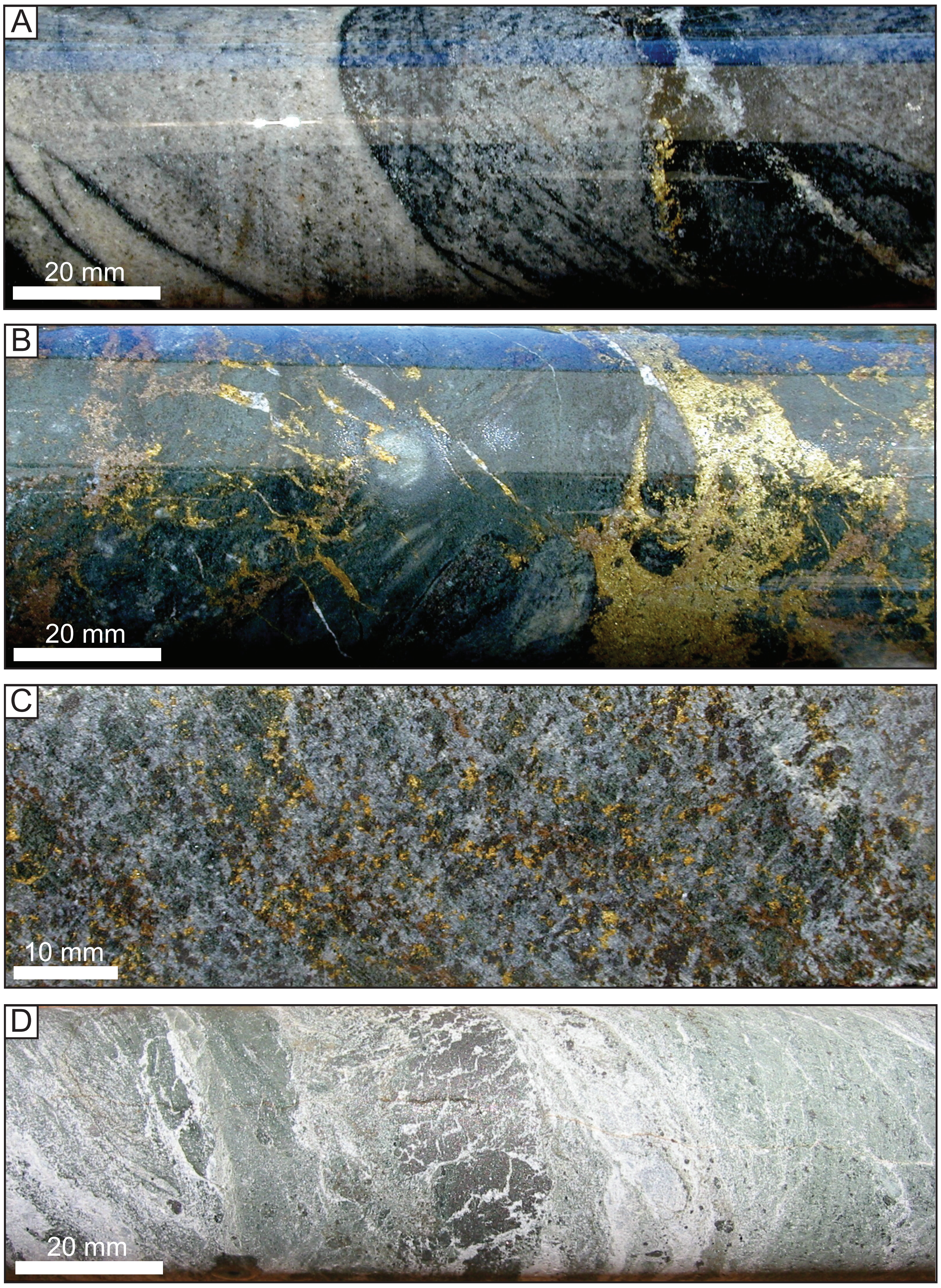

Figure 7.13 Drill core photos from Eloise West. A. Medium grained psammite with early pervasive albite-quartz alteration overprinted by fracture controlled biotite-hornblende (mafic-silicate) alteration and biotite-hornblende-calcite veining. Late-stage chalcopyrite-pyrrhotite fracture infill occurs around mafic-rich veins. B. Chalcopyrite mineralisation with strong retrograde chlorite/actinolite alteration of earlier mafic silicate alteration. Small relict patches of early albite-biotite alteration are preserved. The chalcopyrite and pyrrhotite appears to be fracture infill and replacement. C. Disseminated chalcopyrite mineralisation hosted by intensely carbonate-magnetite-chlorite-actinolite altered host rocks. This sample is located peripheraly to the highly mineralised sample in B. D. Pervasively albitised meta-psammite with intense magnetite-carbonate alteration. Modified from Gow and Little, 2003.

Stage I Albite alteration (Albitisation)

Geochemical analysis of least altered metarkose/metarenite units by Baker (1996) indicated variable Na_2O contents between 2.4 and 4.9 % (3.2 and 6.6% wt. Na) due in part to primary albite/oligoclase grains and variable albite-rich alteration. Baker (1998) documented zones of intense albite alteration of the amphibolite units. Albite-altered amphibolite may contain up to 70-80 % albite resulting in strong enrichment in Al_2O_3 (14.4 - 15.9 wt. %) and Na_2O (2.5 to 5.0 %) in END019 (Fig. 7.14). The TruScan™ results shown in Figs. 7.16 and 7.17 show a similar enrichment in Al and Na in the amphibolite, suggesting intense albitisation of these units in the central region of the deposit. Elevated Sc (Fig. 7.17), V and Ti (not shown) are consistent with a ultramafic-mafic precursor prior to metamorphism and alteration.

On a molar (K/Al vs. Na/Al) diagram (Fig. 7.16) units logged as amphibolite with elevated Al and Na plot towards the Albite-Muscovite field of Davies and Whitehead (2006). The relatively low Fe contents observed in END019 (Baker, 1998; Fig. 7.14) and in the EAM holes (Fig. 7.15-7.17) is likely due to Fe depletion during regional sodic metasomatism across the Mount Isa Inlier (Williams, 1994). Baker (1998) documented depletions in Mg, K and Ca from the amphibolite units during metasomatism, again consistent with observed mass changes associated with Na-metasomatism in the Mount Isa Inlier (de Jong and Williams, 1995). Locally, the amphibolite at Eloise has been sheared and has developed a strong biotite foliation at the eastern boundary (Baker, 1998) and is geochemically characterised by increasing K_2O, MgO and FeO.

The Median Fault (Fig. 7.6) is characterised by displacement of the amphibolite over the meta-arenite units and is accompanied by intense carbonate veining and silicification (Baker, 1998). Fig. 7.14 shows the location of the Median Fault at 180 m depth and a sharp decrease in most major elements except SiO_2 and CaO.

Stage II Mafic overprint

Early albite alteration in the amphibolite, schist and meta-arenite is overprinted by biotite and amphibole as veins and more broadly as wall rock replacements and near shear zones (Baker and Lang, 1998). Geochemically this is identified by elevated Mg, Fe and K in the meta-arenite and schist units (Figs. 7.14 and 7.16). Biotite altered amphibolite, meta-arenite and schist show chemical trends towards igher K/Al molar ratios (Fig. 7.17).

Stage III Quartz - Carbonate

Baker (1996) and Baker and Laing (1998) document a range of carbonate-rich assemblages roadly coincident with brittle-ductile transition deformation related to main-stage Cu-Au mineralisation. The local increase in CaO (Fig. 7.14) may be attributed to calcite-rich veins and breccias. Associated silicification manefests as localised increases in Si, although changes in Si are most noteable where sulphide phases dominate (Fig. 7.14).

Main stage mineralisation

The main stage mineralisation is noted by increased concentration of S, Cu and Fe as the mineralogy becomes dominated by chalcopyrite and pyrrhotite (Fig. 7.12) in the Elrose, Levuka and 40 Lodes (Baker, 1996). Within the Levuka Lode, Si, Al, Ca and Na decrease as Fe increases coincident with elevated Cu and Au (Fig. 7.14; Baker, 1996). The TruScan XRF analysis intercepts similar zones of elevated S, Fe and Cu (Fig. 7.16).

Also coincident with these elements are Zn, Pb and As (Fig. 7.17) which appear to concentrate in the mineralised zone. Zn appears to form a potential halo around the mineralised zone extending into the amphibolite stratigrpahy (Fig. 7.17). This may be related to late stage (Stage IV) calcite-fluorite-sphalerite-galena-arsenopyrite veins with low Cu reflecting the absence of chalcopyrite (Baker, 1996) wThe TruScan highlights an apparent associations between Co and the ore zone although Co concentrations by XRF have not been verified on this dataset. Baker (1996) Identified different associations of Co at Eloise including within pentlandite (high Ni-Co, low As) and cobaltite (high Co and As). The TruScan data shows a broader distribution of Cu (locally up to 5 % Cu) throughout the analysed intervals (Fig. 7.17) including in the amphibolite units in EAM128 and EAM 130. These intervals were not sampled during resource development assays at Eloise (far right hand columns of Fig. 7.17) and suggest a broader distribution of mineralisation than is constrained by current

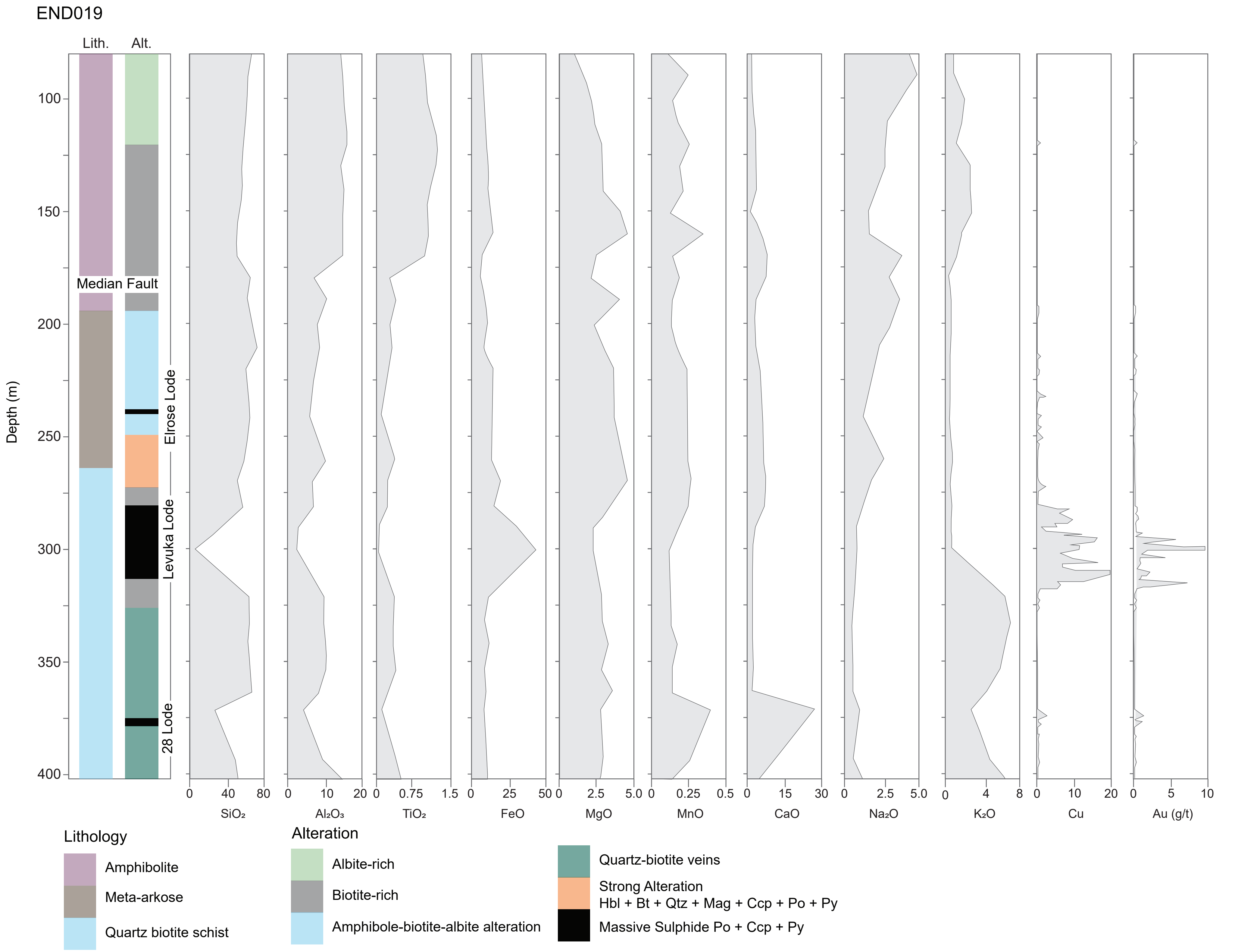

Figure 7.14. Down hole example graphic log from drill hole END019 intercepting Elrose, Levuka and 28 Lodes. Whole rock geochemical assays are shown for selected elements (Modified from Baker, 1996). The sampling interval represents 2 m composites sampled at 10 m intervals. Samples were analysed by XRF and Neutron Activation Analysis.

assay data. The Truscan data is a preliminary release and further examination of these high Cu, low S zones needs to be carried out. Correlations between Au-Ag and Cu are related to the occurrence of electrum and gold within chalcopyrite (Baker, 1996). The alteration system evolved from early Na-Ca feldspar stability during regional albitisation and Ca-metasomatism (Stage I, II) to potassic feldspar stability (stage IV; Baker, 1996). This trend is observed regionally (Williams and Blake, 1993).

ORE MINERALOGY

The mesoscale ore mineralogy at Eloise is dominated by chalcopyrite, pyrrhotite, pyrite and magnetite (Figs. 7.6 to 7.8). Bornite, chalcocite and covellite are rare (Hodkinson et al. 2003).

Trace occurrences of Co (e.g., cobaltite) and Ni bearing phases occur throughout the deposit. Pentlandite is largely associated with pyrrhotite (Baker, 1996) and may be identified by Co-Ni association in the geochemical data with deposit scale zonation from pyrrhotite-poor southern lodes to pyrrhotite-rich northern lodes (Baker, 1996).

Textural evidence by Baker (1996) indicates that magnetite was deposited prior to, and synchronous with, Cu-Au mineralisation where it is commonly also intergrown with pyrrhotite.

Figure 7.13 shows backscattered electron (BSE) images and corresponding classified mineral maps for samples collected and analysed by CSIRO Uncover using a Tescan Mira scanning electron microscope (Glazely et al. 2016). The samples were collected from two drill holes and represent meta-arenite, amphibolite, biotite schist and massive sulphide samples. The samples highlight the overprint of early albite rich alteration in meta-arenite by K-Feldspar and biotite (Fig. 7.13A). Amphibolite dominated by hornblende (Fig. 7.13B) and progressive quartz-plagioclase alteration (Fig. 7.13C). Fabric is largely preserved in biotite schists (Fig. 7.13D and E) but cross cut and altered by chalcopyrite-pyrrhotite and calcite. Main stage mineralisation and fomration of massive sulphide replacements are shown in Figs. 7.13F to H) where massive, texture destructive chalcopyrite overprints and replaces earlier biotite-amphibole (hornblende) alteration.

TIMING OF MINERALISATION

Relative Timing

Baker and Laing (1998) constrained the relative timing of mineralisation at Eloise to broadly coincide with the later stages of the D3 Isan Orogeny (1540-1500 Ma) and correlate this with the regional effects of the emplacement of the Williams Batholith (1540 - 1490 Ma). Mineralisation was associated with both brittle and ductile deformation, brecciation and fracture infill (Baker, 1996) that post-dates peak metamorphism in the Mount Isa Inlier (D2; Beardsmore et al. 1988; Williams and Blake, 1993). The deposit is unconformably overlain by Late Jurassic and Cretaceous sedimentary rocks (Li Shu and Robertson, 2002).

Absolute age-dating

Baker et al. (2001) used radiogenic ($^{40}Ar/^{39}Ar$) methods to constrain the absolute age of pre-mineralisation biotite from a pre- to syn-D_2 vein to 1,555±4 Ma marks the peak regional D_2 metamorphism. Subsequent alteration-mineralisation at Eloise is interpreted to post-date this peak metamorphic event and is variably affected by post-mineralisation thermal resetting (Baker et al. 2001). A geochronological summary is shown below:

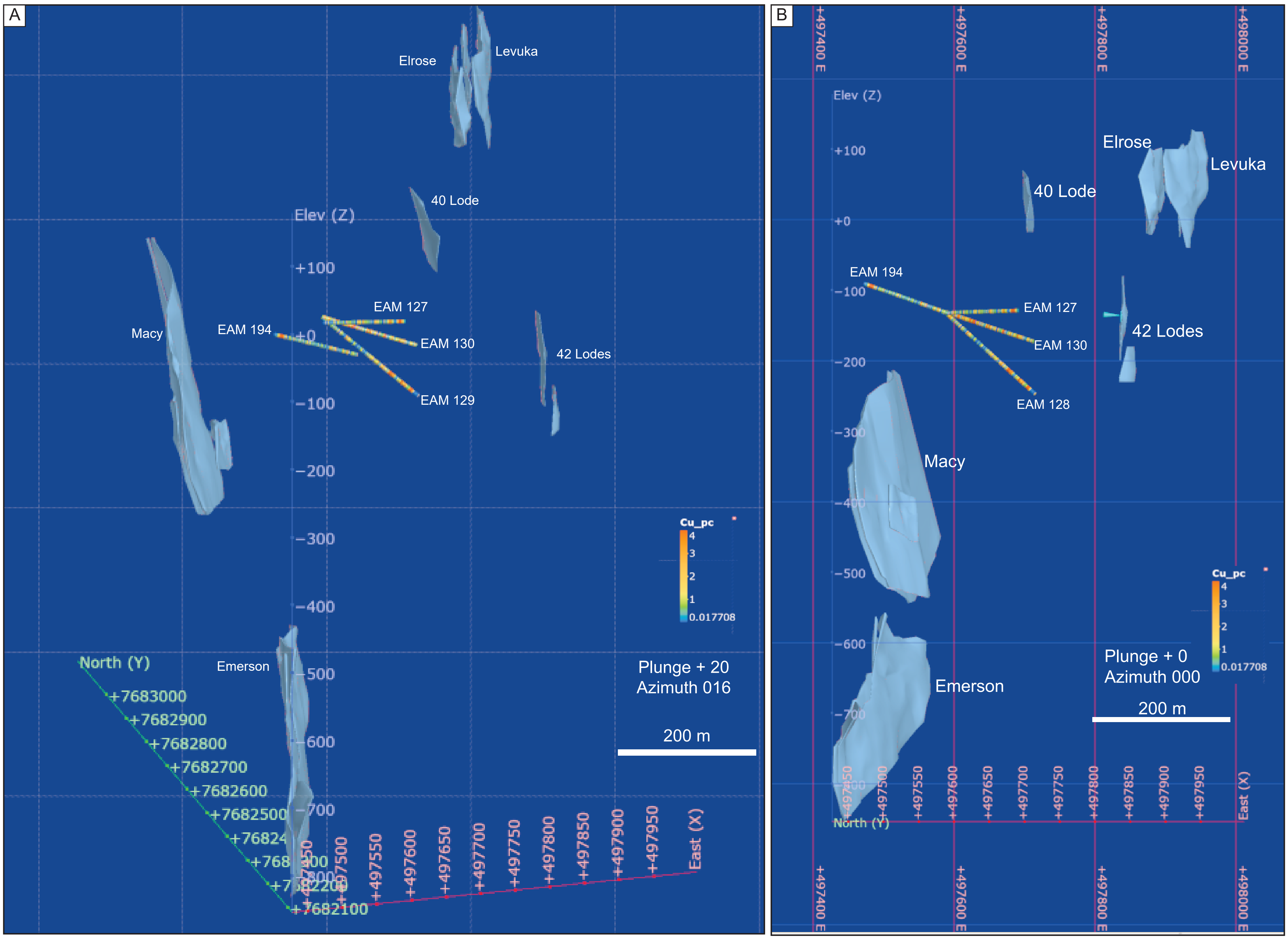

Figure 7.15. Location of drill holes EAM127, EAM128, EAM130 and EAM194 in the central region of the Eloise deposit. A. Oblique view looking NE; B. Sectional view looking North.

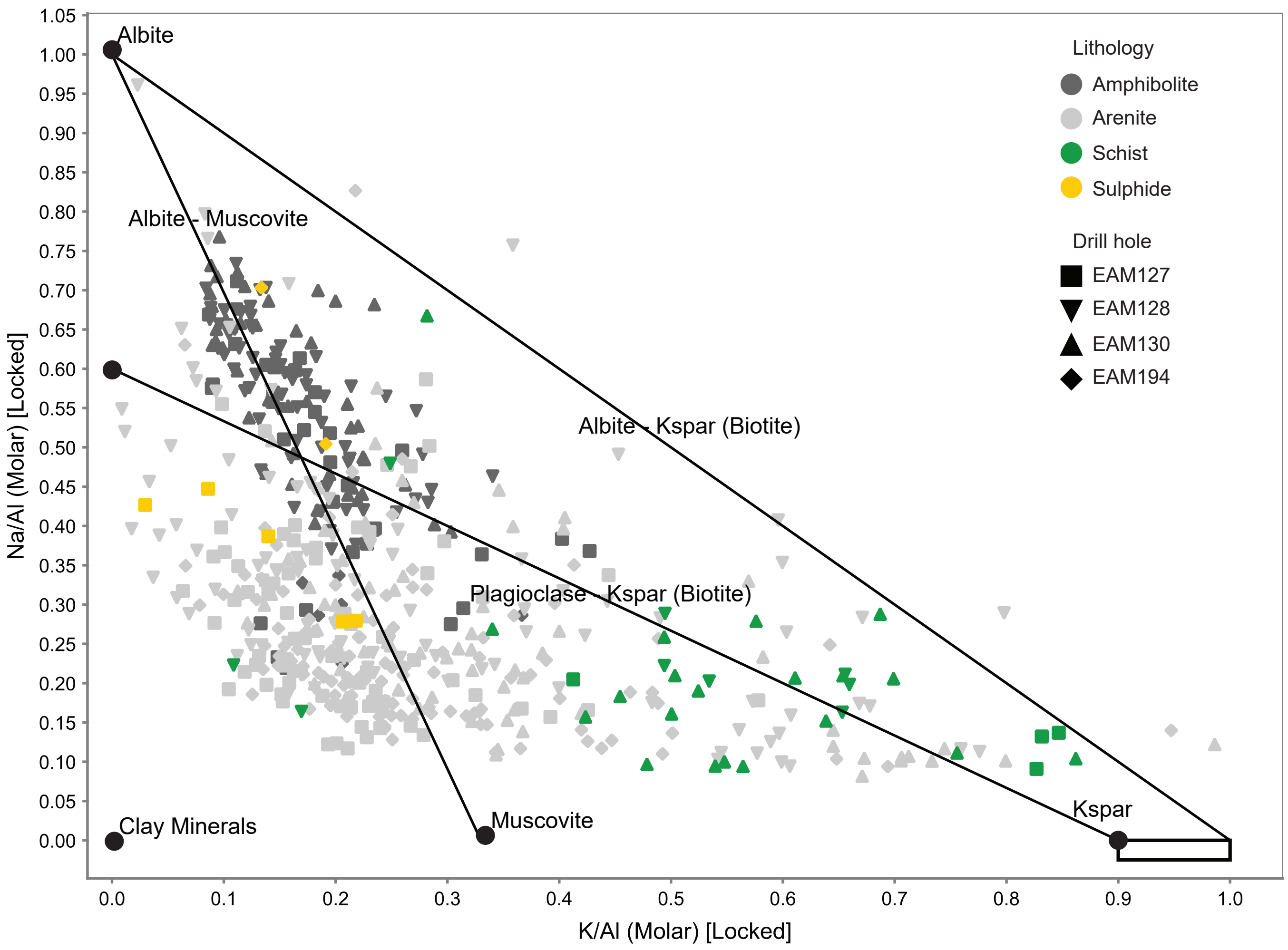

Figure 7.16. Molar ratio plot for K/Al and Na/Al (Davis and Whitehead, 2006) using TruScan™ XRF geochemical data from 4 drill holes at Eloise highlighting the variation in alteration style from albite-rich assemblages in the amphibolite to more biotite- and K-Feldspar-rich assemblages in the schist. The Arenite is variably altered to albite, muscovite and K-Feldspar/biotite.

1) Pre-syn D_2: 1555±4 Ma (early biotite)

2) Stage II: 1530±3 Ma (hornblende)

3) Stage II: 1521±3 Ma (biotite; *NB. possible post-mineralisation thermal resetting*)

4) Post-ore: 1514± 3 Ma (muscovite)

GENETIC MODEL

The formation of the Eloise deposit is broadly consistent with genetic models for iron oxide Cu-Au deposits proposed by Hitzman et al. (1992). In this model, deep seated magmatic hydrothermal fluids follow flow paths dictated by pre-existing structural fabric (folds, faults, cleavage).

Mineralisation at the Eloise deposit is the product of a complex interaction between regionally extensive alteration-deformation events and localised fluid flow across the ductile-brittle transition (Baker and Laing, 1998).

The location of Eloise at a dilational jog in the regionally extensive Levuka Shear Zone appears to have been critical to the structural and hydrothermal evolution of the deposit, partitioning strain into the metamorphised Soldiers Cap Group during regional brittle-ductile events (Baker and Laing, 1998).

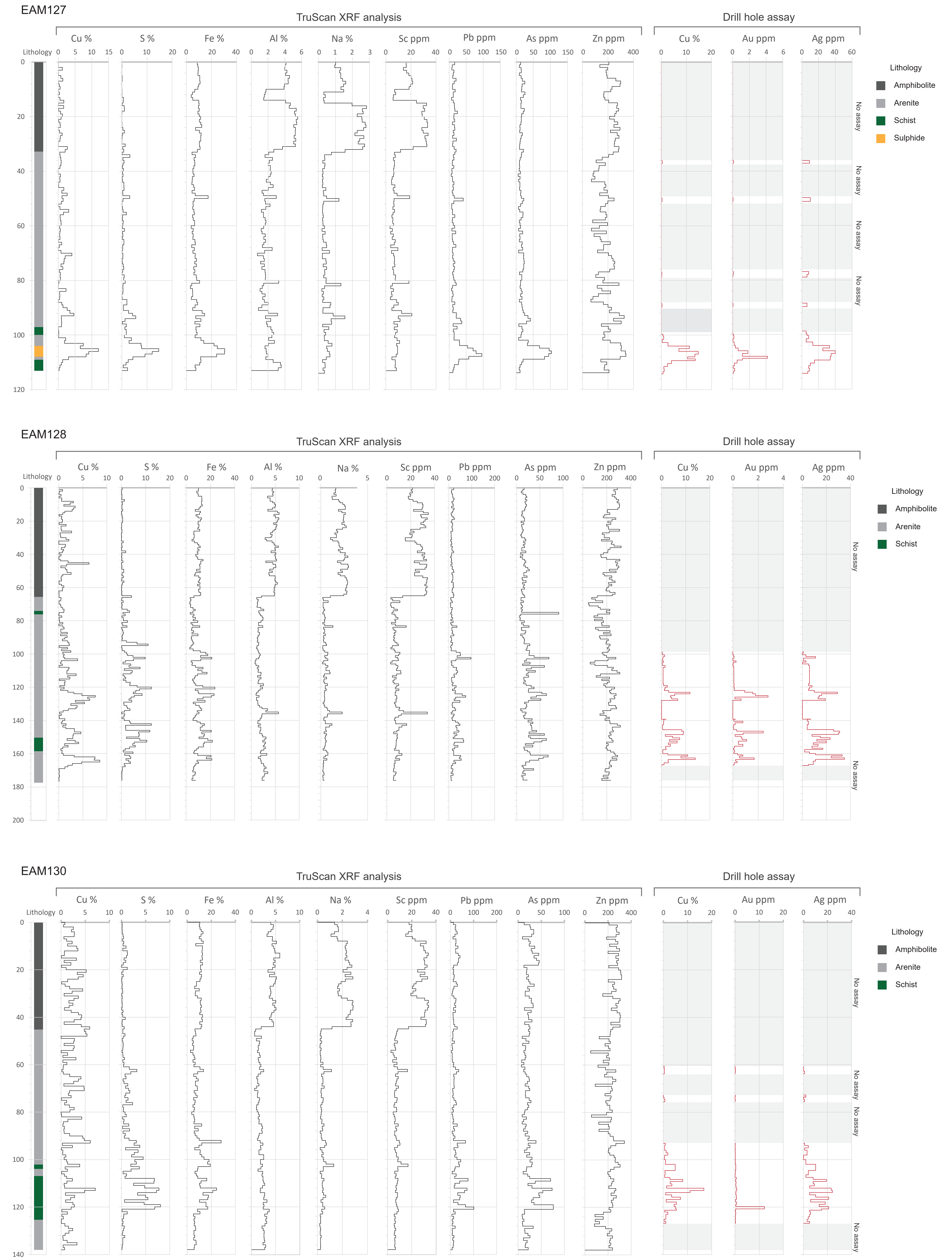

Figure 7.17. TruScan™ analysis for selected elements composited to 1 m interval averages. Lithology is from FMR Investments geological logging together with original assay elements from the drilling data base (note variable assay intervals and no data for some regions of the cores).

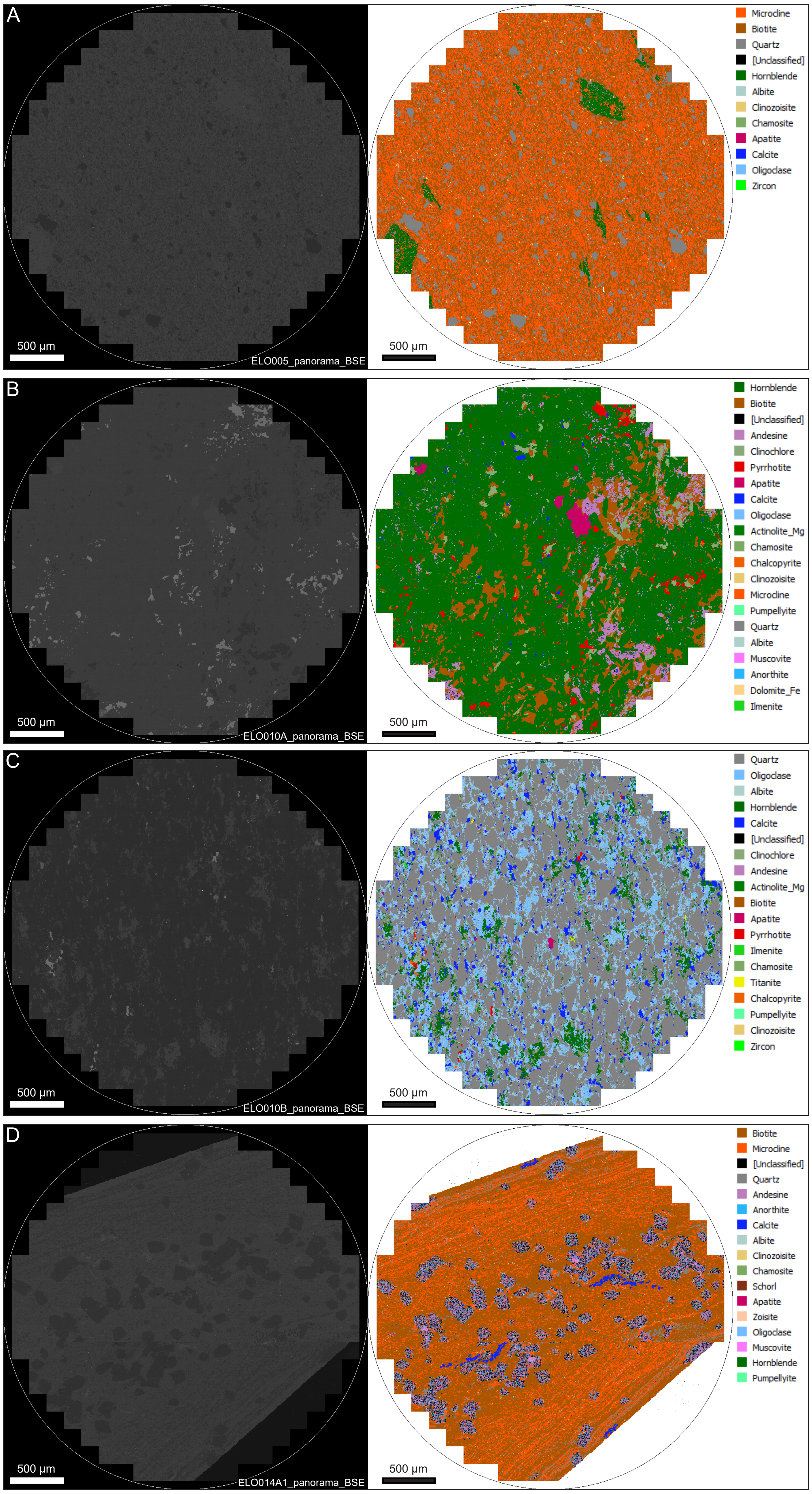

Figure 7.18. Backscattered electron images and corresponding classified mineral maps for samples from Eloise. A. Meta-arenite with K-feldspar-biotite alteration minor (relict) hornblende (ED060-90.58 m). B. Amphibolite dominated by hornblede and biotite intergrown with plagioclase (andesine) chlorite and apatite. Pyrrhotite is diseminated throughout. ED062-32.68. C. Quartz-oligoclase altered amphibolite with minor hornblende (ED062-32.68). D. Biotite schist with pronounced layer parallel fabric of biotite and microcline (K-Feldspar) with relict grains of magnetite-plagioclase and late stage calcite (ED062-89.75).

Fig.	Sample ID	Drill Hole	Depth
A	ELO05	ED060	90.58
B	ELO010A	ED062	32.68
C	ELO010B	ED062	32.68
D	ELO014A1	ED062	89.75
E	ELO014A2	ED062	89.75
F	ELO015A	ED062	95.75
G	ELO015B	ED062	95.75
H	ELO015C	ED062	95.75

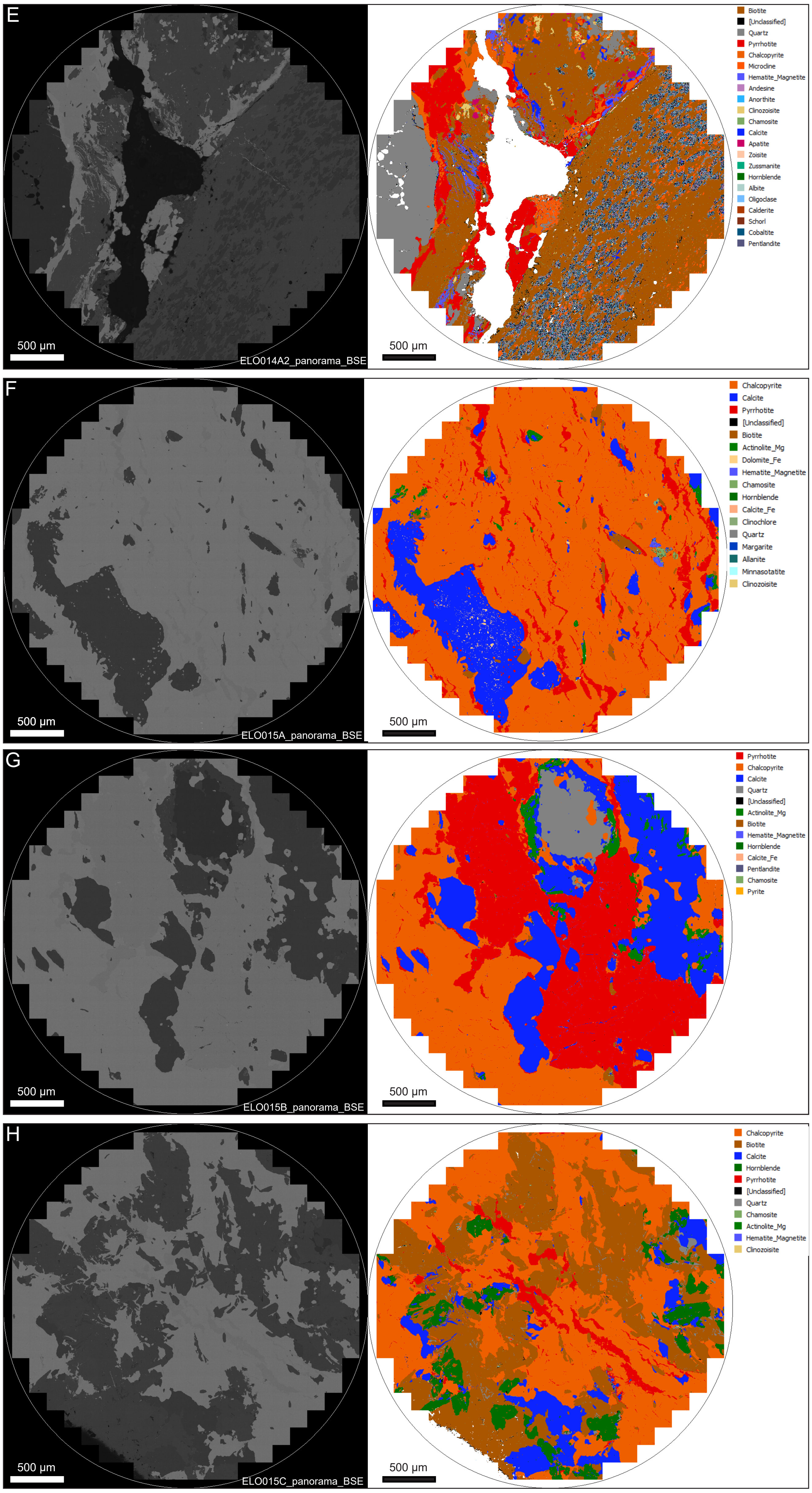

Figure 7.18 cont.

E. Biotite schist with relict grains cross-cut by quartz-pyrrhotite-chalcopyrite-calcite mineralisation (ED062-89.75). F. Massive sulphide mineralisation comprising massive chalcopyrite and pyrrhotite with calcite. Minor biotite (relict) remains as lath-like lozenges (ED062-95.75). G. Massive sulphide mineralisation ith massive intergrown chalcopyrite and pyrrhotite with calcite and quartz (ED062-95.75). H. Massive sulphide (chalcopyrite) overprinting earlier biotite-hornblende (actinolite) alteration and late pyrrhotite veins.

Peak metamorphism in the Eastern Mount Isa block is synchronous with the regional D_2 event (Beardsmore et al. 1988). At Eloise this manefests as S_1 inclusion trails in prograde garnet (Baker and Laing, 1998) during amphibolite facies (550-600ºC) metamorphism (Baker, 1996; Baker and Laing, 1998). Development of a penetrative S_2 cleavage in the Soldiers Cap Group (amphibolite, schist and meta-arenite) occurred during D_2.

Stage I albitiation was related to regionally extensive high temperature (400-500ºC) fluids concentrated along structures within the Levuka Shear Zone (Baker, 1998). Stage II alteration was driven by thermally retrograding (magmatic?) fluids which caused local brecciation of previously albitised units and extensive mafic vein formation, again largely concentrated within pre-existing fabrics and shear zones(Baker and Laing, 1998; Baker, 1998).

Stage III alteration and mineralisation was caused by continued retrograde cooling of these fluids (<450ºC) within the N-NE shear. The fluid flow paths ay have been influenced by existing structures including D3/F3 fold hinges which plunge steeply south, formed during E-W oriented compression (Baker and Laing, 1998). The folds may in part influence the steep plunge of the Eloise Deeps lodes. Concurrent with mineralisation was the onset of brittle deformation forming NW oriented structures (e.g., Median Fault) which also host mineralisation (Baker and Laing, 1998).

EXPLORATION

Discovery Method

Eloise was discovered in 1986 by BHP Minerals during regional exploration for Broken Hill-type mineralisation within the Eastern Mount Isa Block (Hodkinson et al., 2003). The deposit is located 10 km east of the exposed part of the Cloncurry-Selwyn zone and is buried below 50 to 70 m of highly conductive Mesozoic sediments of the Eromanga basin (Brescianini et al. 1992).

The deposit was discovered using moving loop EM (TEM) and fixed loop TEM following the identification of linear aeromagnetic trends in regional datasets (Figs. 7.1 to 7.5; Brescianini et al. 1992).

Magnetic Features

Moderate to high intensity magnetic features with N-S oriented linearity were identified in the aeromagnetic survey. A ground magnetic survey (Fig. 7.19 after Brescianini et al. 1992) shows local complexity and the location of the Eloise magnetic ridge and a zone of carbonate-magnetite veining (up to 30% magnetite). The NNW-trending Middle Fault s interpreted by Brescianini et al. (1992) to occur between the Eloise magnetic ridge and the bullseye anomaly as an inflection in the contour data (Fig. 7.19).

Surface TEM

Surface TEM methods were successful in identifiying the Eloise deposit despite being overlain by highly conductive post-mineralisa-

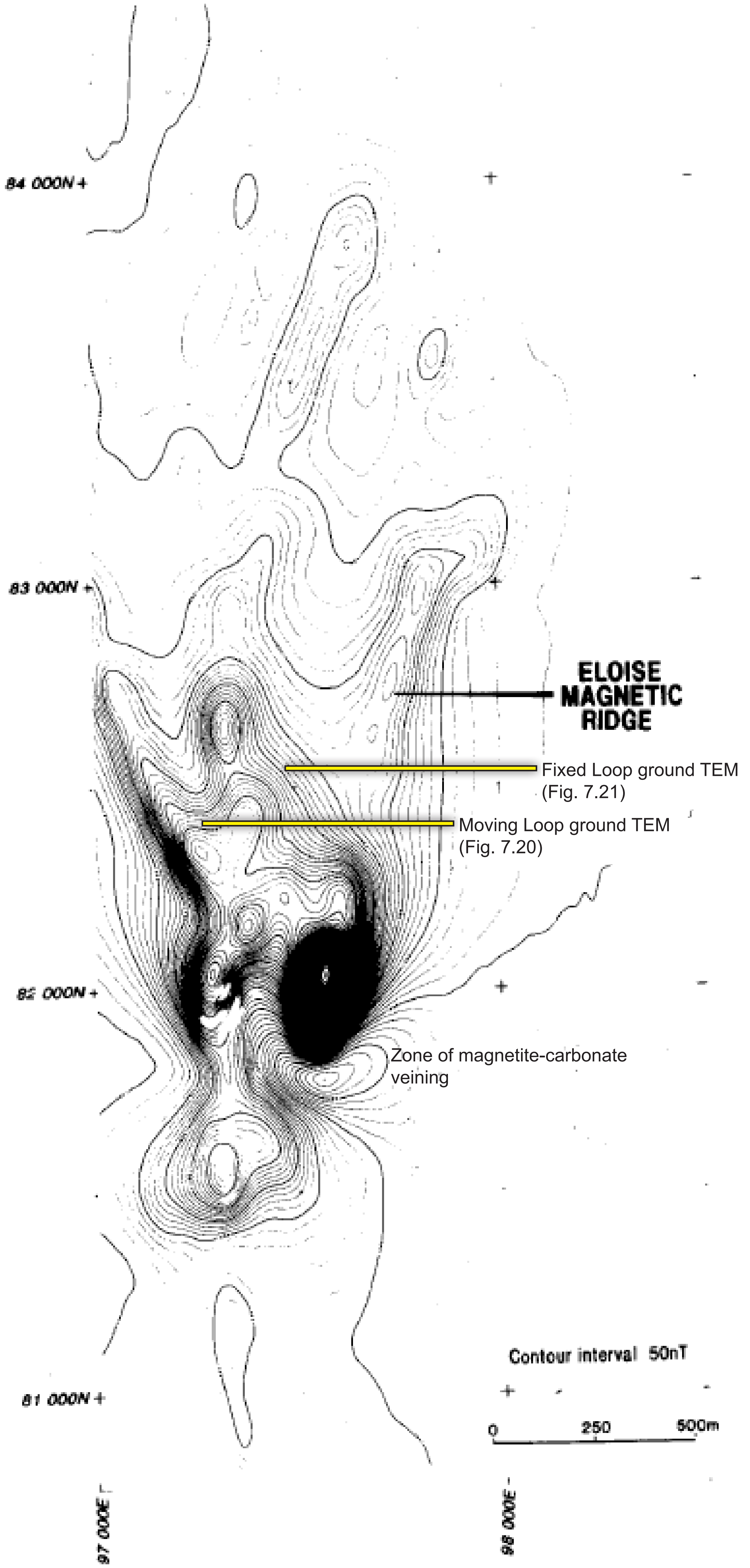

Figure 7.19. Ground magnetic contours (50nT contour intervals) from Brescianini et al. (1992). Coordinates show local mine grid.

tion sediments with typical resistivity of 2 to 4 ohm (Brescianini et al. , 1992). BHP Minerals inplemented a grid based analysis of magnetic anomaly trends using moving-loop TEM. The Eloise depsosit was discovered in Section 82 450N (7,682,589mN) shown in Fig. 7.20. The late time responses coinciding with the surface projection of the Eloise ore body despite gradual thickening of the conductive overburden towards the east (Brescianini et al. 1992).

Figure 7.21 shows the results of a fixed loop TEM survey along section line 82 550N (7,682,689 mN; position of section shown in Fig. 7.19). The response due to mineralisation is evident as an inflection in the late decay response profiles (Brescianini et al. 1992; Fig. 7.21). BHP Minerals' 5th exploration drill hole at Eloise (END17) targeted this feature in Fig. 7.21 and intercepted 20 m of high grade Cu-Au (Brescianini et al. 1991).

Down hole TEM

The down hole TEM survey highlighted the effectiveness of this technique for delineating highly conductive suphidic lenses. The down hole TEM profile for the discovery hole (END17) is shown in Fig. 7.22 after Brescianini et al. (1992) which shows a rise in voltage levels within 10 m of the mineralised lens. The complexity in Fig. 7.22 results from continuously mineralised interval >100 m in length.

Gravity data

A forward gravity model was produced prior to a deposit-scale gravity survey by BHP based on observed/measured density variations measured on drill core (Table 7.3) and modelled geometry of the mineralised lense (Brescianini et al. 1992). The result of the survey is shown in Fig. 7.23 as residual Bouguer gravity contours assuming a near-surface density of 2.2 t/m^3 and a regional surface (3.5 mGal/km) has been removed (Brescianini et al. 1992). These data highlight a positive anomaly (1 mGal aplitude) 500 m north of Eloise with a southern expression of this feature being a ridge that attenuates south of the Middle Fault (Fig. 7.23) due to the presence of sulphide mineralisation and associated alteration.

Resistivity and IP

Brescianini et al. (1992) document a dipole-dipole IP and resistivity survey designed to penetrate the highly conductive overburden. Fig. 7.24 shows there is no anomaly in the apparent resistivity profile which instead highlights the overburden thickness variation. An alteration system is interpreted to be resolvable in the IP decoupled signature (Fig. 7.24).

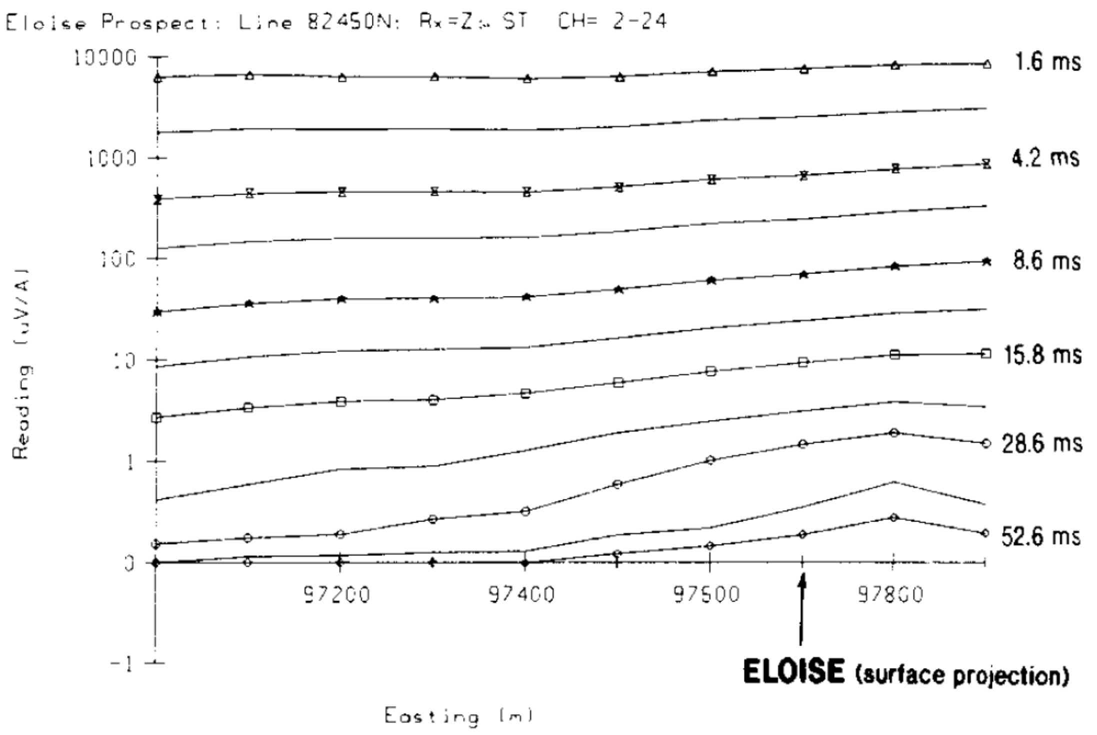

Figure 7.20. Moving loop TEM profile along section 82 450N (7,682,589 mN) showing the surface projection of the Eloise deposit (Brescianini et al. 1992). Coordinates show local mine grid.

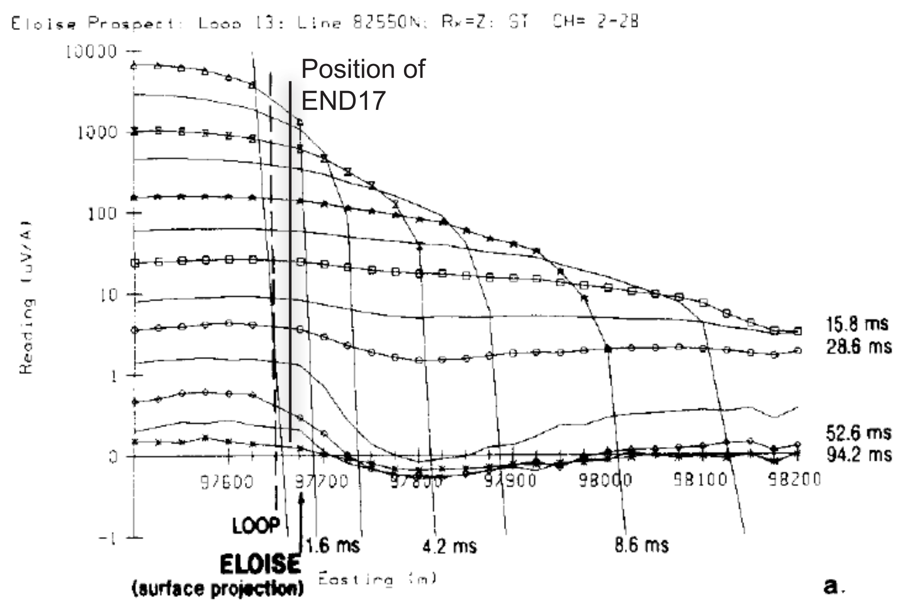

Figure 7.21. Fixed loop TEM profile along section 82 550N (7,682,689 mN) showing the surface projection of the Eloise deposit (Brescianini et al. 1992). Coordinates show local mine grid.

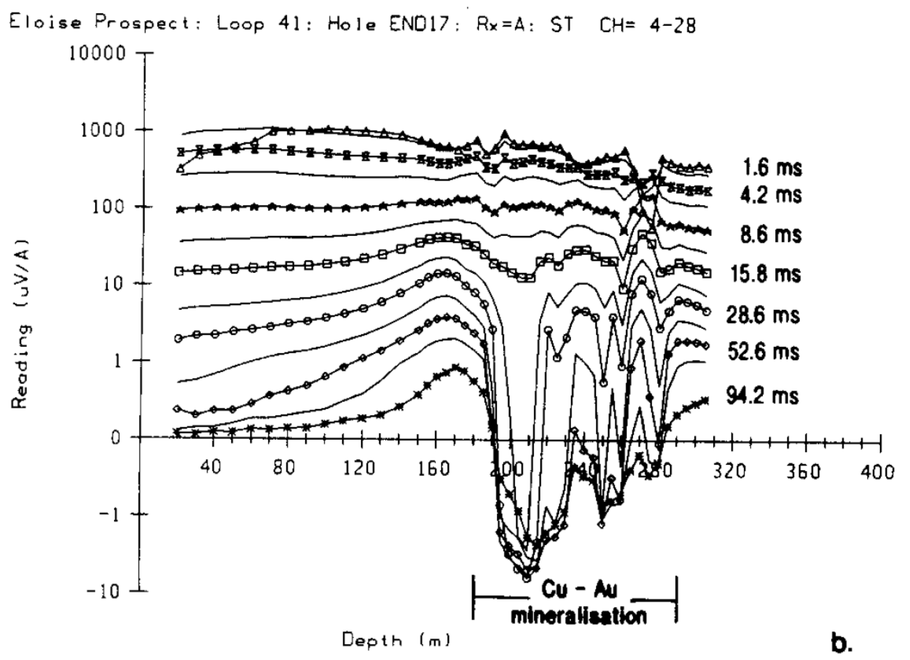

Figure 7.22. Downhole TEM profile for discovery hole END17 (location targeting fixed loop ground TEM feature in Fig. 7.21) showing the rise in voltage from 150 m before a long interval of complexity representing continuously mineralised intersection (Brescianini et al. 1992).

This polarisable zone is centred at 97 500E (497,663mE) in the decoupled data (Fig. 7.24, lower image) and interpreted to represent a broad alteration system (800 m wide) which in in contact with the overburden-basement interface (Brescianini et al. 1992).

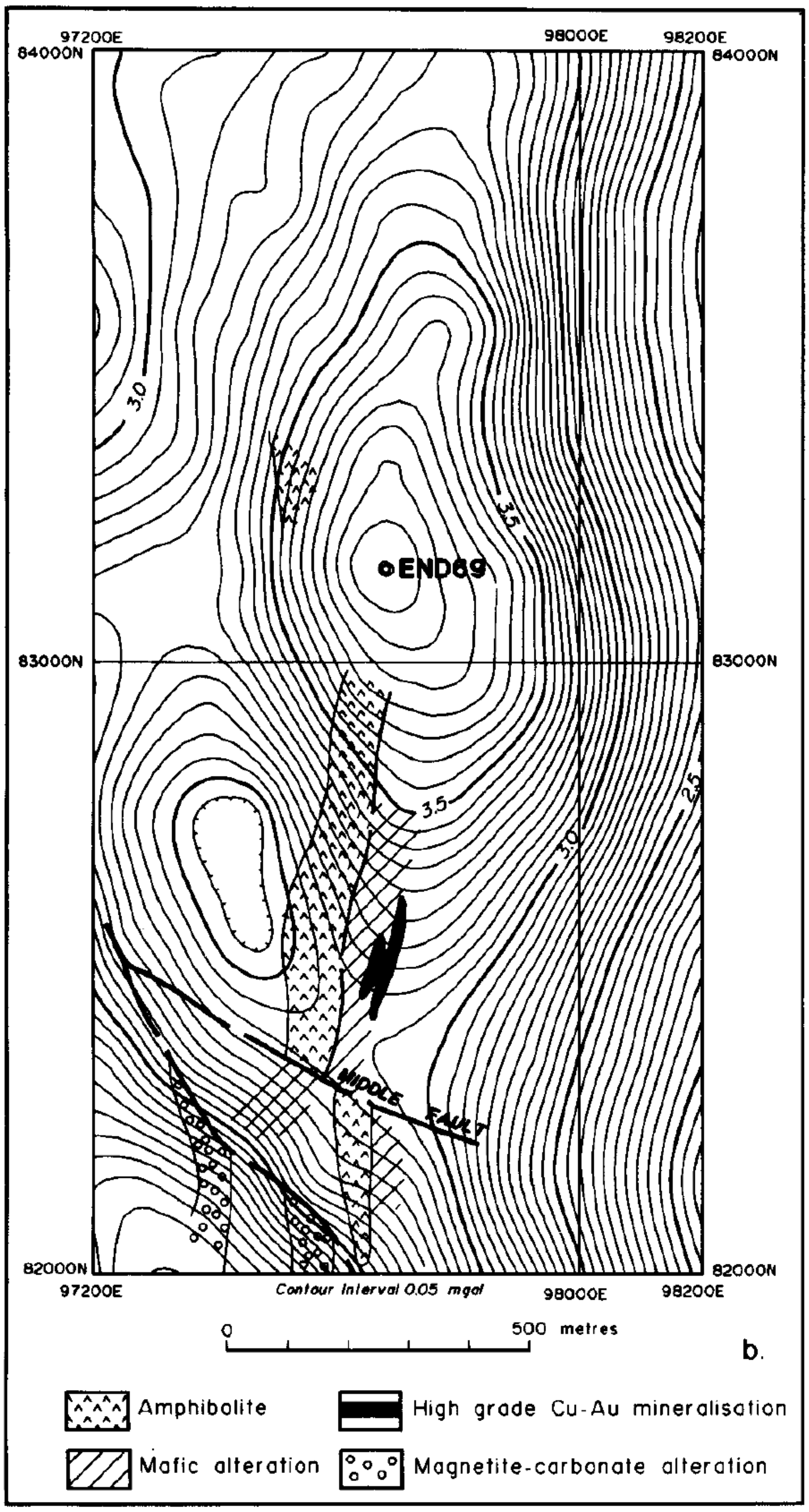

Figure 7.23. Bouguer gravity anomaly contours (1 mGal; Brescianini et al. 1992).

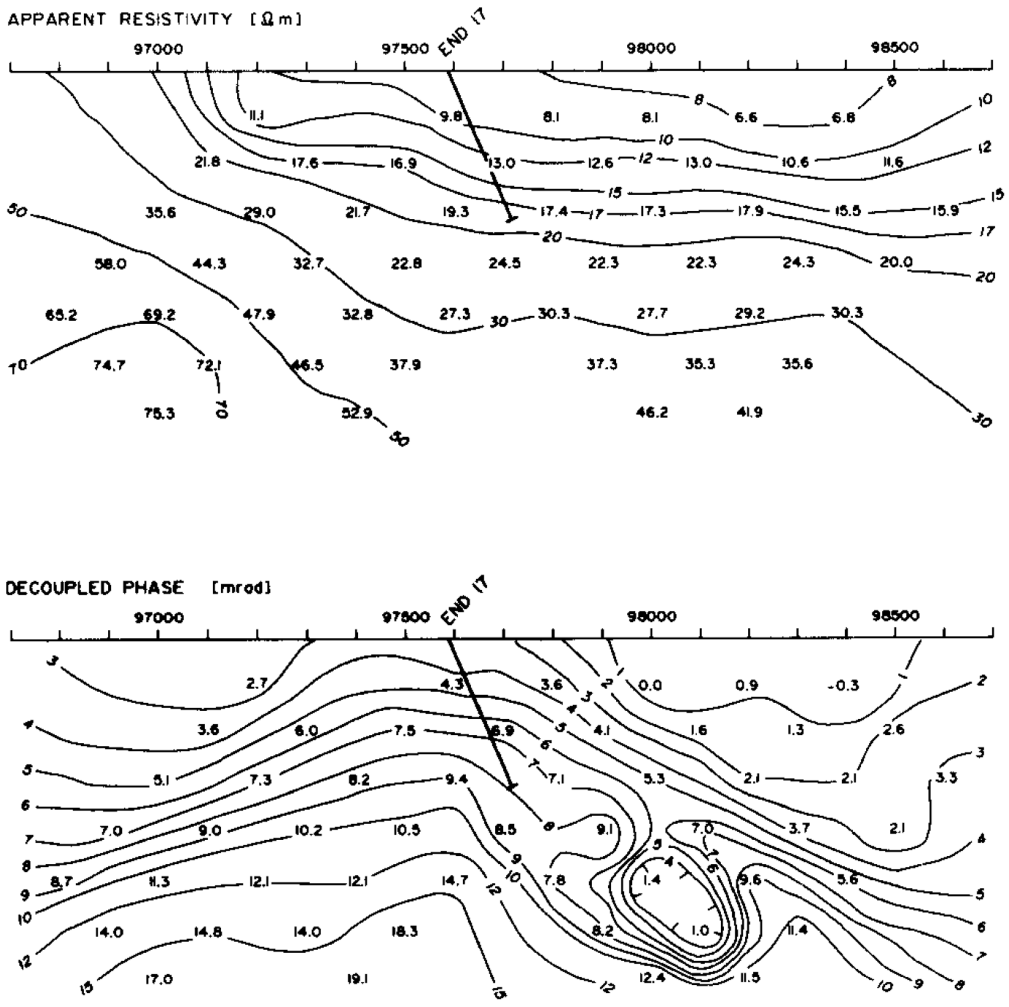

Figure 7.24. Apparent resistivity (upper) and decoupled phase IP (lower) from Brescianini et al. (1992). The discovery hole is shown (END17).

REFERENCES

Baker, T., 1996. The geology and genesis of the Eloise Cu-Au deposit, Cloncurry District, NW Queensland, Australia. PhD Thesis, James Cook University, Townsville.

Baker, T., 1998. Alteration, mineralization and fluid evolution at the Eloise Cu-Au deposit, Cloncurry District, NW Queensland, Australia. Economic Geology 93, 1213-1236.

Baker, T., Perkins, C., Blake, K.L., Williams, P.J., 2001, Radiogenic and stable isotope constraints on the genesis of the Eloise Cu-Au deposit, Cloncurry district, NW Queensland. Economic Geology, 95, 723-742.

Baker, T., Laing, W.P., 1998, Eloise Cu-Au deposit, East Mt Isa Block: structural environment and structural controls on ore. Australian Journal of Earth Sciences, 45, 429-444.

Beardsmore, T.J., Newbery, S.P., Laing, W.P., 1988. The Maronan Supergroup: an inferred early volcanosedimentary rift sequence in the Mount Isa Inlier, and its implications for ensialic rifting in the Middle Proterozoic of northwest Queensland. Precambrian Research 40, 487-507.

Blenkinsop, T., Huddlestoneholmes, C., Foster, D., Edmiston, M., Lepong, P., Mark, G., Austin, J., Murphy, F., Ford, A., Rubenach, M., 2008. The crustal scale architecture of the Eastern Succession, Mount Isa: The influence of inversion. Precambrian Research 163, 31-49.

Breakaway Resources, 2003. Annual Report, 2003. 95p.

Brescianini, R.F., Asten, M.W., McLean, N., 1992. Geophysical characterisation of the Eloise Cu-Au deposit, NE Queensland, Exploration Geophysics 23, 33-42.

Bucher, K.,1994. Petrogenesis of metamorphic rocks, Berlin, Springer Verlag, 318p.

Davies, J.F., Whitehead, R.E. 2006. Alkali-Aluminia and MgO-Aluminia molar ratios of altered and unaltered rhyolites. Exploration and Mining Geology 15, 75-88.

de Jong, G., Williams, P. J., 1995. Giant metasomatic system formed during exhumation of mid-crustal Proterozoic rocks in the vicinity of the Cloncurry Fault, NE Queensland,. Australian Journal of Earth Sciences 42, 281-290.

Edmiston, M., Lepong, P., Blenkinsop, T., 2008. Structure of the Isan Orogeny under cover to the east of the Mount Isa Inlier revealed by multiscale edge analysis and forward and inverse modelling of aeromagnetic data. Precambrian Research 163, 69-80.

Gazely, M., Patterson, B., Austin, J., Godel, B., 2016, UNCOVER Cloncurry - Background on Techniques and Methods. CSIRO Australia, pp.31.

Gow, P., Little, G.A., Eloise Cu-Au mine site visit summary 9 December 2003. X-Strata MIscellaneous report, Unpublished.

Hannan, K., Lilly, R., Tang, J., 2018. The Geochemistry Tool Kit. A geochemical exploration reference for northwest Queensland. Geological Survey of Queensland, Department of Natural Resources, Mines and Energy, Brisbane, 168 pages.

Hinman, M.C., Huisman, D., Little, G., Porter, M., 2018. Solid Geology Interpretation of the Southern Eastern Fold Belt, Mt Isa, Northwest Queensland, Geological Survey of Queensland, Department of Natural Resources, Mines and Energy, Brisbane, 15 pages.

Hitzman, M., Oreskes, N., Einaudi, M.T., 1992. Geological characteristics and tectonic setting of Proterozoic iron oxide (Cu-U-Au-REE) deposits. Precambrian Research, 58, 241-287.

Hodkinson, I., Grimsley, E., Baensch, A. 2003. Eloise Copper Mine Geology - Back to Basics. 5th International Mining Geology Conference, Bendigo, Australia. 17-19 November 2003. p. 1-8.

Laing, W.P., 1998. Structural-metasomatic environment of the East Mt Isa Block base-metal-gold province. Australian Journal of Earth Sciences 45, 413-428.

Li Shu, Robertson, I.D.M., 2002. Surficial geology around the Eloise Cu-Au Mine and dispersion into mesozoic cover from the Eloise mineralisation, NE Queensland. CRC LEME Open File Report 135, pp. 85.

Morse, M.P., Murray, A.P., Williams, J.P. 1992. Gravity anomaly map of Australia. Australian Geological Survey Organisation, scale 1:5,000,000.

Murphy, T., Hinman, M., Donohue, J., Pirlo, M., Valenta, R., Jones, M., Pratt, A., 2017. Deep Mining Queensland: Prospectivity Analysis in the Southern Cloncurry Belt, Queensland, Australia. Geological Survey of Queensland, Department of Natural Resources, Mines and Energy, Brisbane, 125pp.

Page, R.W., Sun, S., 1996. Age and provenance of granites and host sequences in the Eastern Fold Belt, Mount Isa Inlier. James Cook University, Economic Geology Research Unit Contribution 55, 96-99.

Robertson, I.D.M., Li Shu, 2003. Eloise Cu-Au deposit, Cloncurry district, Queensland. CRC LEME, CSIRO Exploration and Mining, Perth. 3pp.

Skrzeczynski, R. 1993. From concept to Cannington: A decade of exploration in the Eastern Succession: Symposium on recent advances in the Mount Isa Block, Australian Institute of Geoscientists Bulletin 13. 35-37.

Spear, F.S., Cheney, J.T., 1989. A petrographic grid for pelitic schists. Contributions to Mineralogy and Petrology, 101, 149-164.

Wallis, D.S., Draper, J.J., Denaro, T.J. 1998. Palaeo- and Mesoproterozoic mineral deposits in Queensland. Australian Journal of Geology and Geophysics 17, 47-59.

Warren, S., Hampton, B., Williams, R., Beattie, E., 2017. Eloise Copper Mine: Then and Now. FMR Investments, Cloncurry IOCG Conference. pp.42.

Williams, P.J., 1998. Metalliferous economic geology of the Mt Isa Eastern Succession, Queensland. Australian Journal of Earth Sciences 45, 329-341.

Williams, P.J., Smith, M.J., 2003. Pb-Zn-(As) enrichments in amphibolites from broken hill-type ore systems, NW Queensland products of retrograde hydrothermal dispersion. Geochemistry - Exploration, Environment, Analysis 3, 245-261.

Wyborn, L.A.I., 1990. Geochemical evolution of the felsic igneous rocks of the Mount Isa inlier and their significance for mineralisation (abs). Mount Isa inlier Geology Conference, Monash University, Melbourne, p6-7.